# Petrographic, palynological and geochemical recognition of dispersed organic matter in the black Anthracosia Shales (Sudetes, south-west Poland)

Grzegorz J. NOWAK[1, *], Anna GÓRECKA-NOWAK[2] and Przemysław KARCZ[1]

[1] Polish Geological Institute – National Research Institute, Lower Silesian Branch, al. Jaworowa 19, 53-122 Wrocław, Poland; ORCID: 0000-0003-2228-5361 [G.N.]; 0000-0002-2932-6851 [P.K.]

[2] Institute of Geological Sciences, University of Wrocław, pl. Maxa Borna 9, 52-204 Wrocław, Poland; ORCID: 0000--0002-1731-7261

We describe the organic petrography, palynology and Rock-Eval pyrolysis values of lacustrine black shales termed the Anthracosia Shales (Upper Carboniferous/Lower Permian) in the Intrasudetic Basin (Sudetes, SW Poland). Samples were taken from cores of two boreholes: Rybnica Leśna PIG 1 and Ścinawka Średnia PIG 1. Maceral composition, miospore assemblage composition, palynofacies and geochemical characteristics of dispersed organic matter in the Anthracosia Shales were used to determine conditions of the environment and to evaluate their petroleum potential. Data from both organic petrography and palynology analyses enabled recognition of three broadly distinct organic associations in these shales: bituminous, humic, and intermediate, while Rock-Eval pyrolysis revealed the presence of bituminous and humic kerogen types I and III. Type I corresponds to the bituminous association, with amorphous organic matter (AOM) dominant in the palynofacies, and type III corresponds to the humic association with phytoclasts prevailing in the palynofacies. The thermal maturity of the organic matter is determined by the values of: (1) vitrinite reflectance $V_{Ro}$ = 0.53–0.73%, (2) palynomorph 3–4 colour index, and (3) $T_{max}$ = 443–447°C, which indicate *oil window* maturity. Some of the TOC results (1.6–2.9 wt.%) indicate that the Anthracosia Shales are good and very good petroleum source rocks, though the thickness of this interval is low (4–5 m). Shales with TOC values <0.5 wt.% prevail, and may be classifed as  poor source rocks.

Key words: Intrasudetic Basin, lacustrine black shales, organic petrography, palynofacies, Rock-Eval pyrolysis, petroleum source rocks.

## INTRODUCTION

Black shales and other organic-rich deposits are common worldwide. Their deposition took place from the Archean to the Holocene. Their role is difficult to overestimate because they are important for geological processes. Being enriched in organic matter, they are considered potential hydrocarbon source rocks, and they may contain important and useful metals. The concentration of organic matter in black shales may play a role in mineralization processes (e.g., Nowak et al., 2001; Oszczepalski et al., 2002; Speczik et al., 2003).

Organic petrography is a significant tool applied in the study of dispersed organic matter in sedimentary rocks due to its importance in exploration for fossil fuel resources (Suarez-Ruiz et al., 2012; Hackley and Cardott, 2016). Depending on thermal maturity level and organic matter composition, black shales are often referred to as sapropelic, bituminous shale, or oil shale. Recognition of such rocks is significant from both geological and economic points of view. They often form source rocks for hydrocarbons and are exploited worldwide (Dyni, 2006; Karnkowski et., 2010; Lin et al., 2013; Sliaupa et al, 2016; Kosakowski et al., 2016; Panja and Velasco, 2018; Mecellari and Whaley, 2019; Mengying and Xinkai, 2021), contributing to economic growth. Widespread geological interest in shale petroleum systems is focused on such rocks as lacustrine shales from various parts of the world (Jadoon et al., 2016; Hackley et al., 2016; Liu et al., 2017; Ghazwani et al., 2019; Goodarzi et al., 2019). In China, it is estimated that more than 85% of hydrocarbon reserves originated in lacustrine settings (Graham et al., 1990; Demaison and Huizinga, 1991; Carrol et al., 1992; Lin et al., 2013; Hackley et al., 2017; Huijuane al., 2018). To estimate hydrocarbon potential, organic geochemistry research is often accompanied by organic petrographic and palynological research, which are useful in the recognition of both the conditions in ancient lakes and the sedimentary processes that led to

* Corresponding author, e-mail: gnow@pgi.gov.pl

the formation of lacustrine shales (Sachsenhofer et al., 2003; Liu et al., 2017; Ghazwani et al., 2019).

Carboniferous/Permian lacustrine shales are common in Central Europe. They occur, for example, in the Bohemian Massif of the Czech Republic (Martinek et al., 2006; Lojka et al., 2009, 2010; Stárková et al., 2015) and in Poland in the Sudetes (Dziedzic, 1959, 1961; Mastalerz and Wojewoda, 1988; Mastalerz, 1990; Mastalerz and Nehyba, 1997). Based on their geological structure, the Sudetes are considered an unpromising region for the occurrence of hydrocarbon deposits. The Anthracosia Shales are known as lacustrine sedimentary rocks occurring in the Intrasudetic Basin in the central part of the Sudetes. These deposits comprise argillaceous, argillaceous-pelitic and argillaceous-carbonate shales (Lorenc, 1993). They are enriched in more or less transformed and altered organic matter, which is responsible for their black or grey colour, allowing them to be recognized as typical black shales. The Anthracosia Shales have not been studied previously to evaluate their value as petroleum source rocks.

Black shales may be considered not only as source rocks for hydrocarbons, but also for metals of economic interest including Au, Cu, Zn, Pb, and Pt (Meyers et al., 1992; Leventhal, 1993). The Anthracosia Shales are characterized by weak copper mineralization; their metallogenic potential was critically evaluated in the early 1950s by Wyżykowski (1954). At the end of the 20th century, more studies on these deposits were made, focused on their sedimentary development, relationship with mineralization, isotopic composition and organic geochemistry (Yawanarajah et al., 1993; Speczik et al., 1995; Mastalerz and Nehyba, 1997). The occurrence, composition, structure and thermal evolution of dispersed organic matter (OM) of the Anthracosia Shales have been studied via organic petrography (Nowak, 1998, 2003, 2007). The results of these studies revealed three associations based on maceral composition. Liptinite, especially macerals of aquatic origin, i.e., alginite and bituminite, are the most abundant components and form a lacustrine sapropelic association, while a humic association consists mainly of terrestrial organic matter. An intermediate association consists of organic components present in both associations. The lacustrine sapropelic association indicates an open-lacustrine environment. The organic composition of the lacustrine sapropelic association is characteristic of type I kerogen. Despite the studies noted above, the knowledge of OM in the Anthracosia Shales in terms of organic petrography characteristics is still insufficient. New data on organic matter of the Anthracosia Shales have been acquired from two boreholes, Rybnica Leśna PIG 1 and Ścinawka Średnia PIG 1, drilled in the eastern part of the Intrasudetic Basin (Fig. 1). In this study, incident-light microscopy was employed to recognize organic matter constituents to establish their distribution in the rocks studied. The study also involved palynological and geochemical research. Such research procedures are commonly applied to determine both the hydrocarbon potential and the depositional environments of potential source rocks (Carvajal-Ortiz and Gentzis, 2018; Ndip et al., 2019; Deaf et al., 2020; Körmösa et al., 2020; Mansour et al., 2020; Mohamed et al., 2020; Abou El-Anwar et al., 2021). We include a discussion of relationships between the content and types of macerals, palynofacies and Rock-Eval data for determination of the hydrocarbon potential of the Anthracosia Shales.

## GEOLOGY

The Intrasudetic Basin (IB) is the largest, NW–SE trending, geological unit in the central part of the Sudetes (Fig. 1A). It represents an intra-montane trough, ~65 km long and 25 km wide. The origin of the IB is related to the Variscan Orogeny in the Sudetes, and its final configuration is the result of late Alpine movements.

Carboniferous, Permian, Triassic, and Upper Cretaceous strata fill the IB and there are numerous stratigraphic gaps and local angular unconformities between them (Nemec et al., 1982; Bossowski et al., 1995). The oldest rocks are of Mississippian age, which initially accumulated under continental conditions, and later in a marine environment. The Pennsylvanian and Lower Permian deposits represent a volcanic-sedimentary succession (Awdankiewicz et al., 2003; Bossowski and Ihnatowicz, 2006). These formed in fluvial and lacustrine environments under progressively drier climate conditions (Bossowski and Ihnatowicz, 1994). This succession is indicated by an increasing frequency of red-brown clastic sedimentary rocks towards the top of the stratigraphic section. These rocks host the lacustrine deposits called the Anthracosia Shales. Their name is related to fossils of the freshwater bivalve genus *Anthracosia*. They occur at the tops of the Ludwikowice and Krajanów formations and they are called the Lower and Upper Anthracosia Shales respectively (Fig. 1B). These shales do not occur in each profile of the Pennsylvanian/Permian sequence, so they do not form laterally continuous units, but rather occur as flat lensoidal bodies with a thickness varying from 20 to 70 m. Their age is still disputed and they are included in the uppermost Pennsylvanian or/and lowermost Autunian (Górecka, 1981; Jerzykiewicz, 1987; Górecka-Nowak, 1989, 1995, 2008; Trzepierczyńska, 1994; Górecka-Nowak and Nowak, 2008). Dunn (2001) also commented on published data from these rocks (Jerzykiewicz, 1987) with respect to palynological studies of rocks from the global stratotype of the Carboniferous/Permian boundary in the Aidaralash Creek in Kazakhstan. These stratigraphic problems are not a concern of this paper and they will be discussed separately.

The Anthracosia Shales consist of alternating grey sandstones and shales (Dziedzic, 1959, 1961; Don, 1961; Miecznik, 1989; Lorenc, 1993; Bossowki and Ihnatowicz, 1994). The former are represented by arkosic siltstones and fine- to coarse-grained sandstones. A clayey or locally marly matrix is typical of these sandstones, which form beds 10–20 cm in thickness. These are interbedded with shales that may transition into other lithologies, e.g., sandy shales and siltstones, and even fine-grained sandstones. Calcareous and marly intercalations also occur. In these rocks, thin coal laminae and thin intercalations of bituminous limestone may also be found. The characteristic feature of these shales is their grey and black colour, due to a relatively high organic matter content. This lithology of the Anthracosia Shales represents an open lake facies (Mastalerz and Nehyba, 1997).

## MATERIALS AND METHODS

Dark grey and black shales were collected from cores of two boreholes – Rybnica Leśna PIG 1 and Ścinawka Średnia PIG 1, drilled in the east of the Intrasudetic Basin (Fig. 1). In the former, the Anthracosia Shales were drilled within a depth interval of 95.0–156.5 m. In the Ścinawka Średnia PIG 1 borehole, the Anthracosia Shales occur within a depth interval of 9.35–108.85 m. Samples of both boreholes were collected from the depth intervals 108.35–143.9 m and 11.35–54.5 m for the Rybnica Leśna PIG 1 and Ścinawka Średnia PIG 1 boreholes, respectively (Fig. 2). They contain fine-grained deposits, mainly shales of grey/black colour with minor fine-grained sandstones. Below these intervals are brown and reddish-brown sandstones
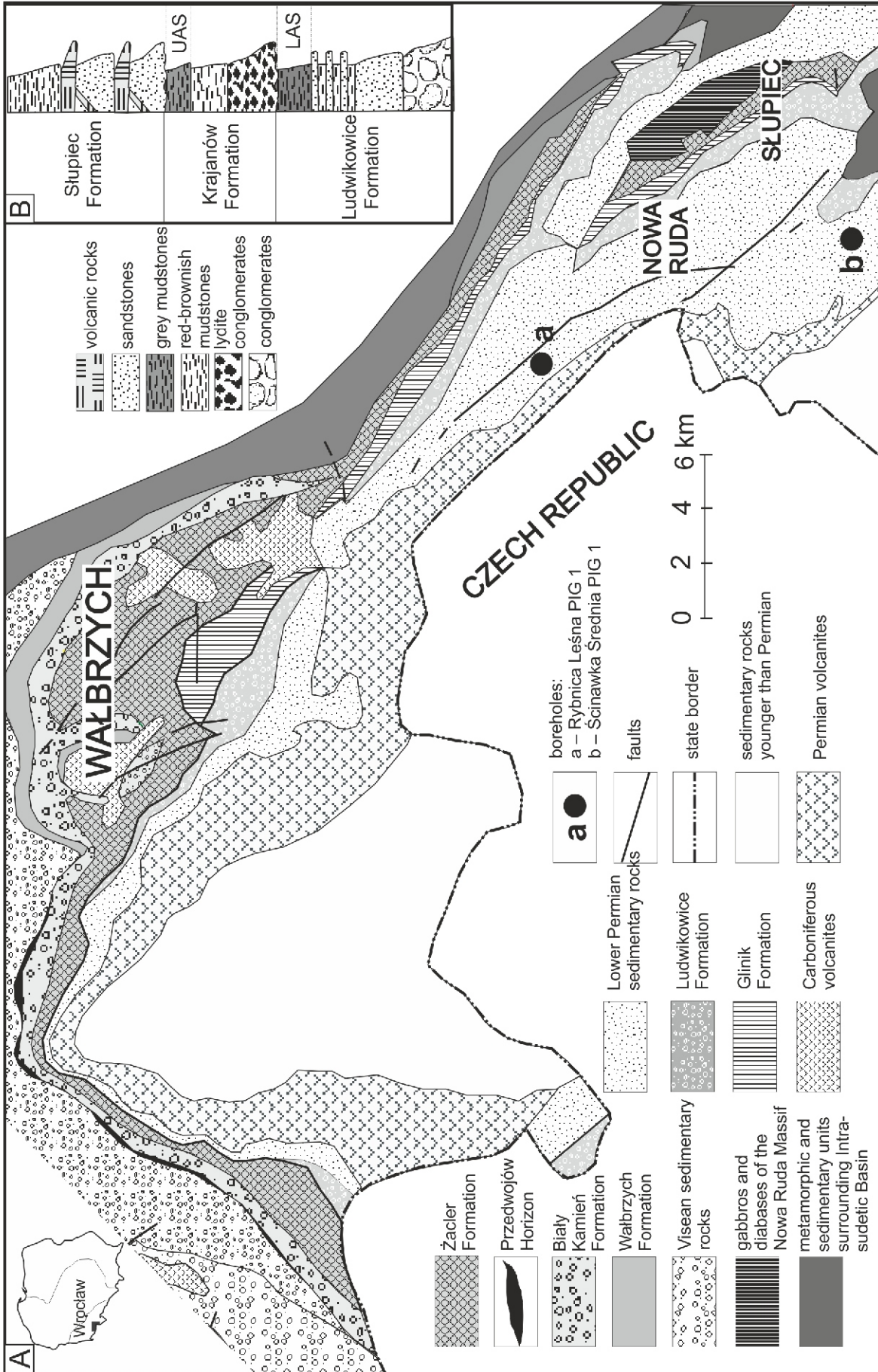
**Fig. 1A – generalized geological map of the Intrasudetic Basin (after Bossowski and Ihnatowicz, 2006, simplified); B – lithostratigraphic position of the Anthracosia Shales among the Pensylvanian/Permian deposits of the eastern part of the Intrasudetic Basin**

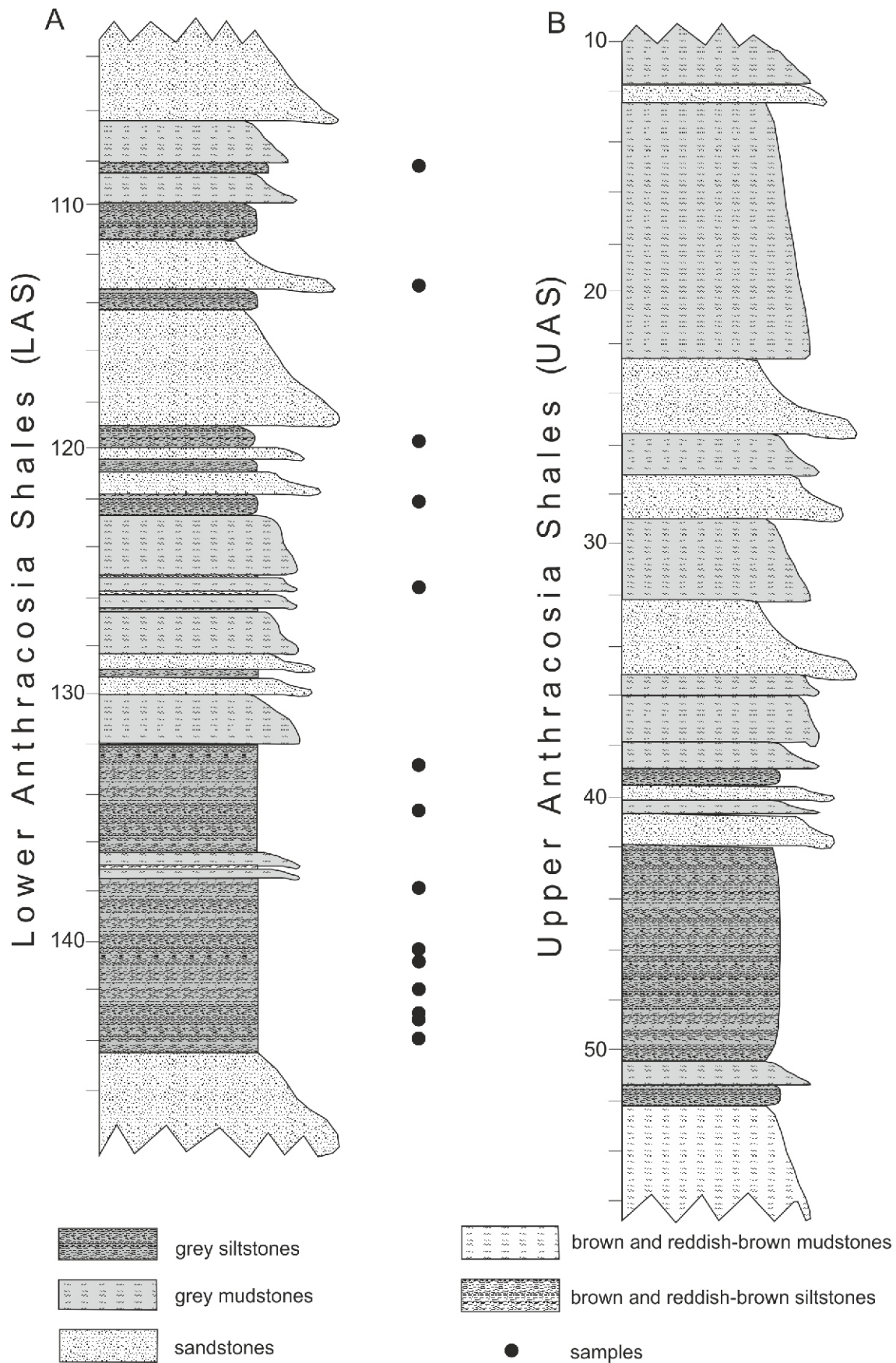LAS – Lower Anthracosia Shales, UAS – Upper Anthracosia Shales

Fig. 2. Lithological sections of the Anthracosia Shales in the profiles studied: A – the Lower Anthracosia Shales in the Rybnica Leśna PIG 1 borehole (the Ludwikowice Formation) and B – the Upper Anthracosia Shales in the Ścinawka Średnia PIG 1 borehole (the Krajanów Formation)

and mudstones, of little value for our research. The total number of microscopically (both petrographically and palynologically) examined samples was 27 (Fig. 2).

The samples were studied using various analytical procedures. The principal methods were optical techniques, making use of both reflected and transmitted light microscopy. Polished surfaces of whole-rock samples cut perpendicular to bedding planes were prepared according to the ISO 7404-2 (2009) procedure and examined under reflected light microscopy. A Zeiss AxioImager 1Am reflected light microscope equipped with UV (with an HBO lamp emitting ultraviolet light, which enabled observations of fluorescence of macerals during irradiation) and white light illumination was used for petrographic observation following widely accepted procedures (e.g., Taylor et al., 1998; Hackley and Cardott, 2016). To study the organic matter, polished sections of the samples were examined under oil immersion at a magnification of 200–500x in reflected white light and fluorescence modes. Maceral quantitative analysis was performed applying the *Zeiss KS RUN 300* point-counted system. On every sample, 250 counts (mineral matter was excluded) were made and the components vitrinite, liptinite, inertinite, solid bitumen and bituminous groundmass were recorded. The maceral terminology used was based on the ICCP System 1994 (ICCP, 1998, 2001) classification and Pickel et al. (2017). Results of the incident light microscopy were applied to determine organic matter composition and to define organic associations (*sensu* Nowak, 2007). Reflectance measurements (random oil immersion) were conducted in reflected light using this same microscope with a 50x objective and the MSP 200 vitrinite reflectance system (J&M GmbH, Germany). The reflectance measurements were taken at 546 nm (monochromatic light). Before the measurements, the microscope was adjusted using sapphire 0.591% *Ro* and yttrium-gallium-garnet 0.905% *Ro* standards. Reflectance measurements were conducted in compliance with the procedures recommended by the International Committee for Coal and Organic Petrology (Stach et al., 1982; Taylor et al., 1998), Hackley et al. (2015) and ISO 7404-5 (2009).

The rock samples for palynological studies were subjected to the standard maceration procedure. Initially they were cleaned and crushed and then processed in acids: hydrochloric acid and then hydrofluoric acid. Each sample was then divided into two parts. The first one, which was intended for palynofacies research, remained unoxidized and was only rinsed and centrifuged. The second part of each sample, intended for sporomorph studies, was oxidized in two oxidants: 65% nitric acid and potassium chlorate. Then this part of the sample was cleaned by multiple washes and centrifuging, and sieved through 16 µm diameter microsieves. Then, microscope slides were made from each part of the sample. The palynofacies and colour of spores were studied on slides made of the unoxidized samples, although sporomorphs were determined on slides made of the oxidized samples. An Optiphot NIKON microscope was used to study the palynological slides. In the course of the palynofacies analysis the palynological particle classification system according to Tyson (1995) modified by Mendonça et al. (2012) was applied and 250–300 particles from each sample were counted. The sporomorphs were observed in terms of their preservation and colour, indicating the degree of thermal maturity. The sporomorph colour was assessed on the Lycospora specimens using the 7 level scale of Batten (1982, 1996).

To examine the petroleum potential (PP), total organic carbon content (TOC), kerogen type, and thermal maturity, the Rock-Eval pyrolysis technique, obligatory for the petroleum exploration industry, was applied to 30 samples of mudstone and claystone from both the Rybnica Leśna PIG 1 and Ścinawka Średnia PIG 1 boreholes. The technique is described widely in petroleum geological literature, the basic characteristics being given by Espitalié et al. (1977). The Rock-Eval measurements were performed using a Rock-Eval 6 apparatus in the most common operating mode (Bulk Rock method, Basic cycle), which is intended for fundamental pyrolytic characterization of rock samples. The method is used for basic screening of all types of rock samples and allows determination of the full set of the Rock-Eval parameters necessary to distinguish between poor and excellent petroleum source rocks. The pyrolysis technique involves thermal decomposition of rock samples (35–100 mg) in pyrolysis and oxidation cycles at a range of temperatures, 300–650°C and 300–850°C, respectively (Lafargue et al., 1998). In the pyrolysis cycle, the samples were first heated in a nitrogen atmosphere at 300°C to release the S1 (mg HC/g rock) fraction, made of volatile compounds (free hydrocarbons). This stage was followed by heating the samples to 650°C to release the S2 fraction (residual petroleum potential). The S1 and S2 fractions were measured by a flame ionization detector, while the S3 fraction ($CO_2$ realeased during pyrolysis) was measured by infrared spectroscopy. The S2 fraction (mg HC/g rock) represents the products of kerogen cracking and the S3 fraction (mg $CO_2$/g rock) derives from oxygen-containing components. In the second part of the analysis, the samples were heated in an air atmosphere from 300 to 850°C to release carbon monoxide and carbon dioxide from the residual and unproductive organic matter and mineral matter. All the results from pyrolysis and oxidation were used to calculate indices: production index (PI), hydrogen index (HI, mg HC/g TOC), oxygen index (OI, mg $CO_2$/g TOC), total organic carbon (TOC, wt.%), mineral carbon (MinC, wt.%) and the maximum temperature $T_{max}$ (°C). The full set of these parameters supports characterization of the type of organic matter, its thermal maturity and petroleum potential.

## RESULTS

### ORGANIC PETROGRAPHY

The vitrinite reflectance ($V_{Ro}$) of the shales under study ranges between 0.53 and 0.73%. A relatively diverse composition of organic matter is found in the Anthracosia Shales from both the Rybnica Leśna PIG 1 and Ścinawka Leśna PIG 1 boreholes. The organic matter is represented by macerals of three groups: vitrinite, liptinite, and inertinite. Additionally, solid bitumen and a mineral-bituminous groundmass were observed in the shales.

Vitrinite macerals occur commonly in the Anthracosia Shales in both borehole profiles, consisting mainly of vitrodetrinite and recognizable larger collotelinite and collodetrinite fragments, which can form microlayers, lenses and larger grains of vitrinite (Fig. 3A,B). Vitrinite is often composed of vitrodetrinite of small size. It has various shapes; a rounded shape indicates transport and redeposition, i.e., a recycled (reworked) type of vitrinite. Its colour is light grey, lighter in shade than the grey colour of the primary vitrinite occurring in the same sample. The primary vitrinite dominates some samples. Its content ranges over wide intervals of 8–100 vol% and 3–95 vol% for the Rybnica Leśna PIG 1 and Ścinawka Średnia PIG 1 boreholes, respectively (Tables 1 and 2), whereas the content of recycled vitrinite does not exceed 2 vol% in either profile. Some samples studied consisted mainly of small vitrinite particles or/and small inertinite pieces (Fig. 3C), which form a kind of humic debris (db; Fig. 3D). Moreover, hydro-
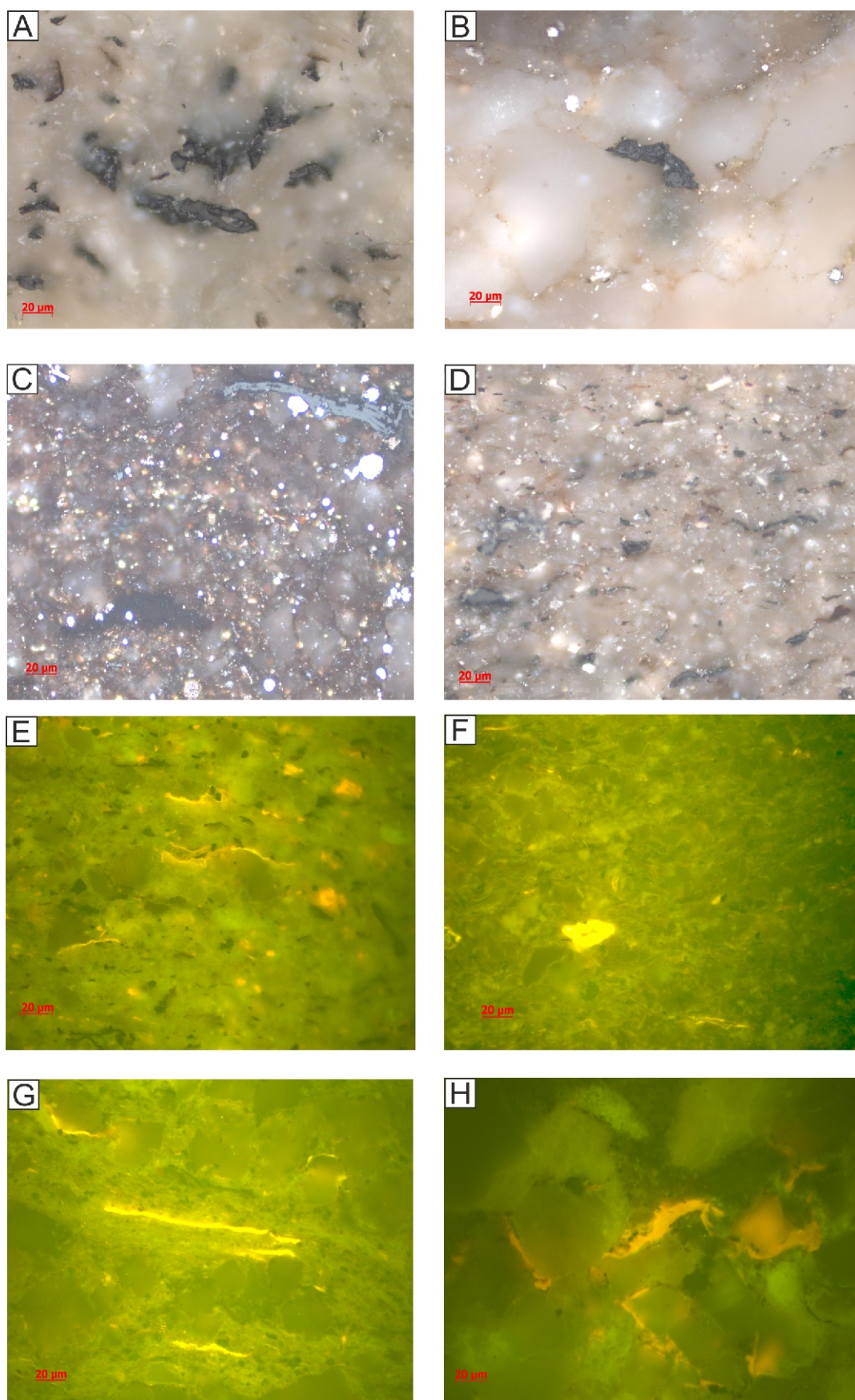
**Fig. 3. Photomicrographs of organic matter in samples of the Anthracosia Shales, taken in reflected white light mode (A–D), incident fluorescence light (E–H)**

**A** – abundant vitrinite fragments – humic association, Rybnica Leśna PIG 1 borehole, depth 108.35 m; **B** – vitrinite in a mineral matrix – humic association, Ścinawka Średnia PIG 1 borehole, depth 30.20 m; **C** – "dark vitrinite" and semifusinite and pyrite – bituminous association, Ścinawka Średnia PIG 1 borehole, depth 54.50 m; **D** – concentration of humic debris – humic association association, Rybnica Leśna PIG 1 borehole, depth 121.80 m; **E** – lamalginite, sporinite and liptodetrinite (all yellow in colour), and non-fluorescing humic matter, Ścinawka Średnia PIG 1 borehole, depth 49.80 m; **F** – telalginite, liptodetrinite of yellow fluorescence colour in bituminite groundmass (bituminous association), Rybnica Leśna PIG 1 borehole, depth 142.85 m; **G** – lamalginite in bituminous-mineral matrix (bituminous association), Ścinawka Średnia PIG 1, depth 45.60 m; **H** – intergranular solid bitumen of yellow fluorescence colour, Ścinawka Średnia PIG 1, depth 50.50 m

**Maceral contents (vol.%) and vitrinite reflectance measurements of the Anthracosia Shales samples from the Rybnica Leśna PIG 1 borehole**

| No. | Depth [m] | V | L: | Sp | Al | Bt | Lpd | IN | Re | BMM | SB | Ro [%] |
|-----|-----------|-----|-----|-----|-----|-----|-----|-----|-----|-----|-----|--------|
| 1 | 108.35 | 95 | 2 | 2 | – | – | tr | 2 | 1 | – | – | 0.53 |
| 2 | 113.20 | 98* | tr | tr | – | – | tr | 2 | tr | – | – | 0.57 |
| 3 | 119.50 | 96* | 1 | 1 | – | – | tr | 3 | tr | – | – | 0.59 |
| 4 | 121.80 | 97* | – | tr | – | – | – | 3 | tr | – | – | 0.60 |
| 5 | 125.50 | 100* | – | – | – | – | – | – | – | – | – | 0.62 |
| 6 | 132.70 | 88 | 6 | 5 | – | tr | 1 | 3 | 1 | – | 2 | 0.67 |
| 7 | 134.60 | 90 | 7 | 6 | – | tr | 1 | 2 | tr | – | 1 | 0.73 |
| 8 | 137.70 | 89 | 8 | 6 | – | 1 | 1 | 2 | tr | – | 1 | 0.62 |
| 9 | 139.90 | 85 | 12 | 7 | – | 2 | 3 | 1 | tr | 1 | 1 | 0.62 |
| 10 | 140.25 | 82 | 13 | 7 | | 2 | 4 | 1 | tr | 2 | 2 | 0.62 |
| 11 | 141.90 | 16 | 75 | 3 | 5 | 63 | 4 | 2 | – | 6 | 1 | 0.63 |
| 12 | 142.85 | 11 | 81 | 3 | 7 | 68 | 3 | 1 | – | 6 | 1 | 0.64 |
| 13 | 143.00 | 10 | 82 | 2 | 6 | 71 | 3 | 2 | | 6 | | 0.61 |
| 14 | 143.90 | 8 | 84 | 3 | 8 | 71 | 2 | 1 | – | 5 | 2 | 0.58 |

Maceral contents determined by point counting; vol.%: volume percent (mineral-matter-free); V – vitrinite; L – liptinite: Sp – sporinite, Al – alginite, Bt – bituminite, Lpd – liptodetrinite, SB – solid bitumen, BMM – bituminous-mineral matrix; IN – inertinite; Re – recycled vitrinite; Ro -

**Maceral contents (vol.%) and vitrinite reflectance measurements of the Anthracosia Shales samples from the Ścinawka Średnia PIG 1 borehole**

| No. | Depth [m] | V | L: | Sp | Al | Bt | Lpd | IN | Re | BMM | SB | Ro [%] |
|-----|-----------|-----|-----|-----|-----|-----|-----|-----|-----|-----|-----|--------|
| 1 | 11.85* | 95* | 2 | 1 | – | – | 1 | 3 | – | – | – | 0.57 |
| 2 | 25.80* | 93* | 4 | 3 | – | – | 1 | 3 | tr | – | – | 0.59 |
| 3 | 30.20 | 94* | 3 | 3 | – | tr | – | 3 | tr | – | – | 0.60 |
| 4 | 32.80 | 93* | 4 | 4 | – | tr | – | 2 | 1 | – | – | 0.61 |
| 5 | 39.50 | 93* | 3 | 3 | – | – | – | 1 | tr | – | 3 | 0.63 |
| 6 | 40.20 | 57 | 28 | 6 | 8 | 8 | 6 | 6 | 2 | 6 | 1 | 0.64 |
| 7 | 42.00 | 59 | 27 | 5 | 8 | 7 | 7 | 4 | 1 | 7 | 2 | 0.63 |
| 8 | 43.60 | 61 | 27 | 3 | 4 | 17 | 3 | 5 | 1 | 5 | 1 | 0.57 |
| 9 | 44.85 | 13 | 60 | 4 | 5 | 44 | 7 | 4 | tr | 21 | 2 | 0.53 |
| 10 | 45.60 | 7 | 72 | 4 | 6 | 61 | 1 | 2 | – | 18 | 1 | 0.62 |
| 11 | 49.80 | 4 | 78 | 2 | 7 | 65 | 4 | 1 | – | 15 | 2 | 0.60 |
| 12 | 50.50 | 3 | 77 | 1 | 7 | 67 | 2 | 1 | – | 17 | 2 | 0.59 |
| 13 | 54.50 | 12 | 70 | tr | 4 | 62 | 4 | 2 | tr | 15 | 1 | 0.65 |

Explanations as in Table 1

gen-enriched vitrinite was found in several samples of high-quality shale (Tables 1 and 2). This type of vitrinite is called "dark vitrinite" (ICCP, 1998; Fig. 3C). Fluorescence colour and intensity vary within the vitrinite macerals dispersed in the shales studied. Vitrodetrinite and collotelinite do not fluoresce under ultraviolet light. However, collodetrinite shows weak, dark brown fluorescence. "Dark vitrinite" can also show brownish and brown fluorescence.

Liptinite macerals are important in the organic matter composition of the Anthracosia Shales. These constituents are relatively abundant in some samples. Liptinite percentages in the shales of the Rybnica Leśna PIG 1 and Ścinawka Średnia PIG 1 boreholes range from 1 to 84 vol% and from 2 to 70 vol%, respectively (Tables 1 and 2). Liptinite in the shales consists mainly of alginite, bituminite, sporinite, and liptodetrinite (Fig. 3E–G). Alginite appears to be an important and numerous maceral in the shales, represented by two varieties. One variety is recognized as telalginite. This type of alginite is formed by discrete algal bodies of both discoidal and elliptical shape. The more abundant alginite type is lamalginite. Generally, lamalginite is relatively difficult to recognize or it is indistinguishable in reflected white light. However, in UV light, lamalginite shows yellow fluorescence. In the Anthracosia Shales of both boreholes, lamalginite forms single elongate laminae or microbands of laminae. The content of alginite is <8 vol% of the organic fraction in the rocks studied (Tables 1 and 2).

The samples show a high content of bituminite, regarded as one of the most important oil-generating macerals. Bituminite is a structureless, purely organic constituent occurring as typical amorphous organic matter. Bituminite can occur in the shales under study as lenticels, irregular microlayers, and concentrations of undefined shapes. It can also occur as single forms in the mineral background as well as coating mineral surfaces. The bituminite content is up to 71 vol% of the organic matter composition (Tables 1 and 2). In microscopic images under reflected white light, it is difficult to distinguish, because it is dark grey with a brownish shade. However, when bituminite is irradiated with UV light, it shows relatively low fluorescence intensity, dark yellow to brown in colour (Fig. 3F, G).

Sporinite is represented chiefly by thin-walled miospores. In microscopic images, it presents mainly as single sporinite forms, often visible within the bituminous-mineral groundmass or mineral matrix. The fluorescence colours of this maceral vary from dark yellow to light orange, significantly darker than the alginite. Sporinite is a component of primary importance among the organic constituents of these shales, with concentrations up to 7 vol% (Tables 1 and 2).

Liptodetrinite can be identified only in UV light, based on a variety of fluorescence properties. Both varieties are represented: (1) algal detritus (sometimes it can be recognized by its residual shape and uniform structure) and (2) sporinite fragments. Liptodetrinite shows yellow to pale orange colours. It is fairly common in the rocks studied (Tables 1 and 2).

The inertinite macerals content does not exceed 7 vol% in the shales studied (Tables 1 and 2). Inertinite consists chiefly of inertodetrinite, but larger fragments can be sometimes recognized as both fusinite and semifusinite cell walls (Fig. 3C). Small pieces of inertinite are commonly associated with vitrinite fragments, together forming humic debris. Inertinite does not display fluorescence and has the highest reflectance of all macerals identified in the Anthracosia Shales.

As well as these macerals, the shales also contain other components of lipid organic matter, predominantly secondary thermally altered organic matter – solid bitumen (SB). These types of organics occur in some of the samples, mainly in those where lipid material is prevalent in the organic matter composi-

tion (Tables 1 and 2). In the shales described here SB is a negligible component, comprising up to 2 vol% of the organic matter composition. These types of organics occur in some of the samples, mainly in those where lipid material is prevalent in the organic matter composition (Tables 1 and 2). Solid bitumen in the shales can sometimes demonstrates intense yellow fluorescence (Fig. 3H).

The liptinite macerals and solid bitumen described above may appear in the shales analysed not only as easily recognizable individual components, but they may also form complexes with other constituents. Liptinite macerals, especially bituminite, may combine with other lipid organic matter to form a natural matrix composed of submicroscopic organic particles and mineral matter. Therefore that type of organic-mineral combination is termed here a bituminous-mineral matrix (BMM). Because of its bituminous character, showing fluorescence properties, UV microscopy allows relatively easy recognition of this type of OM (Fig. 3G). This material occurs mainly in those shale samples in which bituminite is very abundant. The BMM contents are up to 21 vol% (Tables 1 and 2).

## PALYNOFACIES AND SPOROMORPH ASSEMBLAGES

The palynofacies observed in the rocks studied consist of three groups of organic particles: phytoclasts, sporomorphs and amorphous organic matter (AOM). These components occur in various proportions.

Phytoclasts are an important and frequent group of organic particles. The content of phytoclasts varies, from 3 to 100% (Tables 3, 4 and Figs. 4, 5). Most of the phytoclasts are opaque, usually black (Fig. 6). They have various outlines – equant, lath or corroded. Non-opaque (translucent) phytoclasts are rather rare but diverse. They were divided into four groups - non-biostructured and biostructuded phytoclasts, membranes and cuticules were found (Tables 3 and 4). The phytoclast size is variable, but usually they are not larger than 50 μm. In some samples phytoclasts are significantly larger, often exceeding 200 μm, sometimes reaching 300 μm. These larger phytoclasts were observed in the Rybnica Leśna PIG 1 borehole profile (depths 132.7137.7 m and 108.35 m).

Amorphous organic matter is a constant and important component occurring in various amounts, up to 97% in each of the profiles studied (Tables 3, 4 and Figs. 4, 5). It occurs as brown or grey-brown opaque matter forming granular aggregates in palynological slides (Fig. 6). Most samples studied contain AOM that coexists with phytoclasts. In some of the samples the amount of AOM is particularly high and here phytoclasts are usually rare. Such a palynofacies composition was observed in the lower parts of both profiles (Tables 3, 4 and Figs. 4, 5). The amount of AOM decreases upwards in both profiles, the abundance of phytoclasts increasing in the same direction. The amount of amorphous matter is relatively low in the samples from the upper parts of both profiles and phytoclasts are very abundant there.

Miospores, belonging to sporomorphs, are the only palynomorph group found and both spores and pollen grains occur in the rocks studied. As palynofacies components they are rather sparse and their content does not exceed 7% (Tables 3, 4 and Figs. 4, 5). However, because of their importance, the sporomorphs have been studied and determined on the slides after oxidation. The state of miospore preservation is variable. Poor preservation is related mainly to pyritization, which is the main destructive factor beside mechanical destruction. Miospore preservation varies from fairly good to very poor. Three levels of preservation have been established: fairly good – only a small part of the miospores shows traces of pyritization

T a b l e  3

**Palynofacies composition (%) of the Anthracosia Shales samples from the Rybnica Leśna PIG 1 borehole**

| No. | Depth [m] | Phytoclasts | | | | | | | AOM | Spores |
|---|---|---|---|---|---|---|---|---|---|---|
| | | Opaque | | | Non-opaque (translucent) | | | | | |
| | | lath | equant | corroded | non-biostructured | cuticle | membrane | bio-structured | | |
| 1 | 108.35 | 36 | 42 | 16 | 1 | – | 1 | – | 2 | 2 |
| 2 | 113.20 | 45 | 40 | 14 | – | – | 1 | – | – | – |
| 3 | 119.50 | 41 | 48 | 10 | – | – | – | – | – | 1 |
| 4 | 121.80 | 46 | 41 | 12 | 1 | – | – | – | – | – |
| 5 | 125.50 | 48 | 36 | 15 | – | – | – | 1 | – | – |
| 6 | 132.70 | 25 | 54 | 10 | 2 | – | 1 | 2 | – | 6 |
| 7 | 134.60 | 33 | 47 | 11 | – | 1 | – | 1 | 2 | 5 |
| 8 | 137.70 | 33 | 40 | 16 | 1 | – | 1 | 1 | 2 | 6 |
| 9 | 139.90 | 49 | 29 | 12 | – | – | – | 2 | 1 | 7 |
| 10 | 140.25 | 37 | 42 | 13 | 1 | – | – | 1 | – | 6 |
| 11 | 141.90 | 3 | 28 | 18 | 1 | – | – | – | 48 | 2 |
| 12 | 142.85 | 10 | 3 | 8 | – | – | – | – | 78 | 1 |
| 13 | 143.00 | 6 | – | – | – | – | – | – | 91 | 3 |
| 14 | 143.90 | 8 | – | 2 | – | – | – | – | 86 | 4 |

T a b l e  4

**Palynofacies composition (%) in the Anthracosia Shales samples from the Ścinawka Średnia PIG 1 borehole**

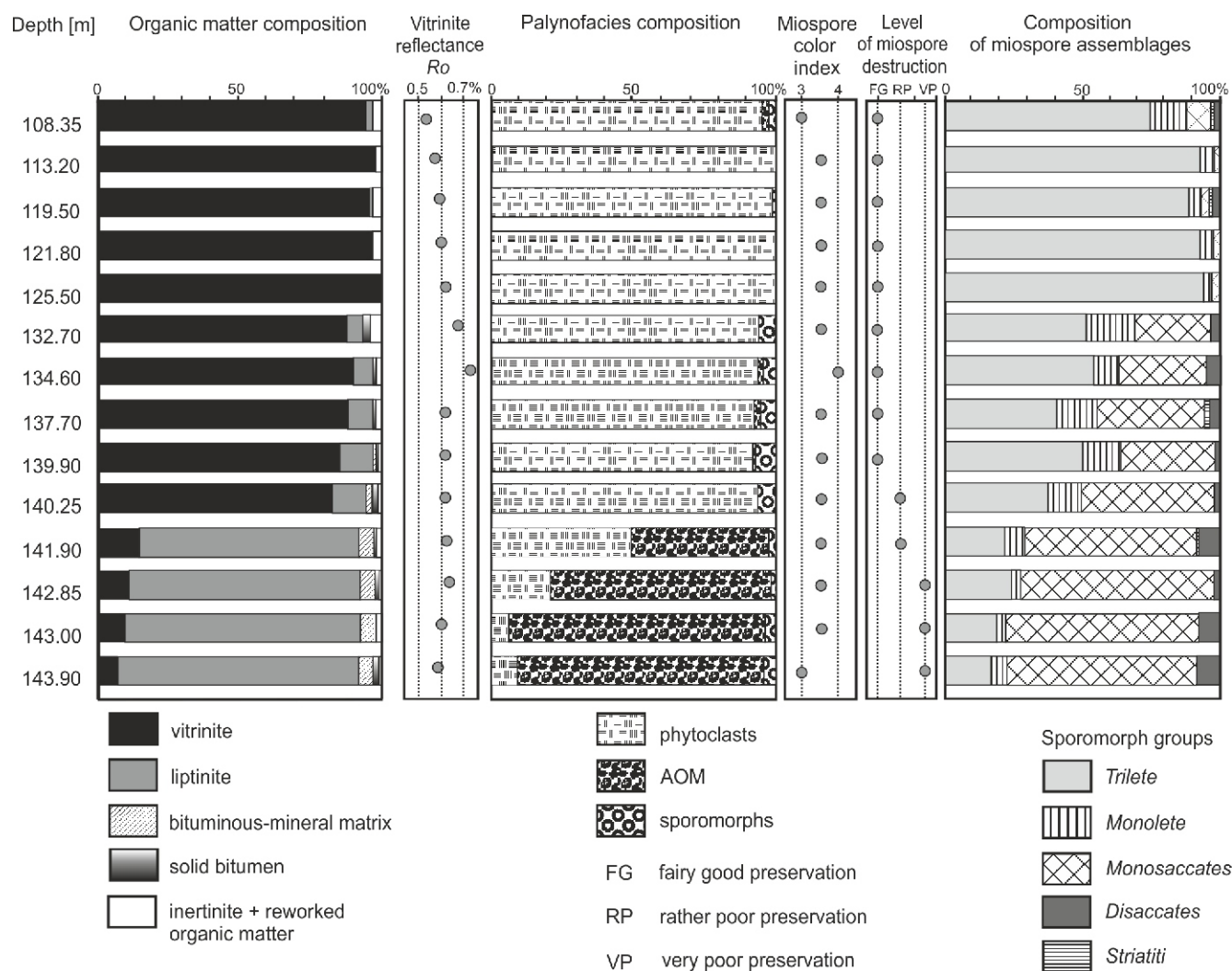| No. | Depth [m] | Phytoclasts | | | | | | | AOM | Spores |
|---|---|---|---|---|---|---|---|---|---|---|
| | | Opaque | | | Non-opaque (translucent) | | | | | |
| | | lath | equant | corroded | non-biostructured | cuticle | membrane | bio-structured | | |
| 1 | 11.85 | 9 | 63 | 17 | 1 | – | – | 3 | 4 | 3 |
| 2 | 25.80 | 9 | 68 | 14 | 2 | 1 | – | 1 | 3 | 2 |
| 3 | 30.20 | 40 | 38 | 15 | – | – | 1 | 1 | 2 | 3 |
| 4 | 32.80 | 37 | 44 | 10 | 2 | – | – | 2 | 1 | 4 |
| 5 | 39.50 | 38 | 40 | 18 | 1 | – | – | 1 | – | 2 |
| 6 | 40.20 | 14 | 26 | 24 | 2 | – | 1 | 2 | 26 | 5 |
| 7 | 42.00 | 20 | 18 | 16 | 4 | 1 | 4 | 7 | 24 | 6 |
| 8 | 43.60 | 14 | 22 | 16 | 5 | 2 | 3 | 6 | 27 | 5 |
| 9 | 44.85 | 6 | 11 | 4 | 2 | – | 3 | 4 | 66 | 4 |
| 10 | 45.60 | 4 | 2 | – | – | – | – | – | 92 | 2 |
| 11 | 49.80 | 3 | 1 | – | – | – | – | – | 96 | – |
| 12 | 50.50 | 2 | – | 1 | – | – | – | – | 97 | – |
| 13 | 54.50 | 4 | 3 | 2 | – | – | – | – | 91 | – |

**Fig. 4. Organic petrography and vitrinite reflectance vs. palynofacies of the Rybnica Leśna PIG 1 borehole**

and mechanical destruction; mostly poor – a significant part of the miospores shows traces of pyritization and mechanical destruction; very poor – most of the miospores show traces of pyritization and mechanical destruction (Figs. 4 and 5). The preservation varies in each profile and depends on the degree of pyritization, which correlates well with the content of AOM. The degree of pyritization is generally the highest in the lower parts of both profiles, where amorphous matter is also very abundant. Samples from the upper parts of both profiles provided slightly better preserved miospores, which are usually free of pyritization traces.

The miospore assemblages are taxonomically diverse and 73 miospore genera were determined there. They were divided into four systematic groups: *Triletes, Monoletes, Monosaccites, Disaccites*, together with the *Striatiti group*. The first of these consists of a diverse assemblage of nearly 50 miospore genera, representing mainly ferns, sphenopsids and lycopsids. The most common in this group are *Angulisporites, Calamospora, Candidispora, Convolutispora*, *Crassispora, Cyclogranisporites*, *Densosporites*, *Dictyotriletes*, *Endosporites*, *Granulatisporites*, *Lycospora*, *Leiotriletes*, *Punctatisporites* and *Verrucosisporites*. The *Monoletes* group is less diverse and include *Laevigatosporites*, *Punctatosporites*, *Spinosporites*, *Thymospora* and *Torispora*. Miospores belonging to this group

were also produced by ferns. The *Monosaccites* group consists of *Cordaitina*, *Florinites*, *Guthörlisporites*, *Potonieisporites*, *Nuskoisporites*, *Schulzospora*, *Wilsonites*, while the *Disaccites* group included *Gardenasporites*, *Hamiapollenites*, *Illinites*, *Limitisporites*, *Pityosporites and Vesicaspora*. Two genera, *Vittatina* and *Hamiapollenites*, were included in the *Striatiti* group. This division of miospores is also important taking into account differences of miospore transportation. Spores from the *Triletes* and *Monoletes* groups were transported mainly by water, while pollen grains, with one or two air bladders, were wind-transported.

All these groups of miospores were distinguished in assemblages associated with all the palynofacies studied, but their content varies (Figs. 4 and 5). Two of the miospore groups, *Triletes* and *Monosaccites*, dominate some samples, reaching 75% of the assemblage. The increase of frequency of one is accompanied by a reduction in the other. The content of the remaining miospore groups, *Monoletes, Disaccites* and *Striatiti,* is significantly lower. On the other hand, the variability in the composition of miospore assemblages in both profiles shows a constant trend with an upwards-increasing *Triletes* group content. The *Monoletes* group in not so numerous and its content shows no clear stratigraphical trend. A decrease in the pollen grain
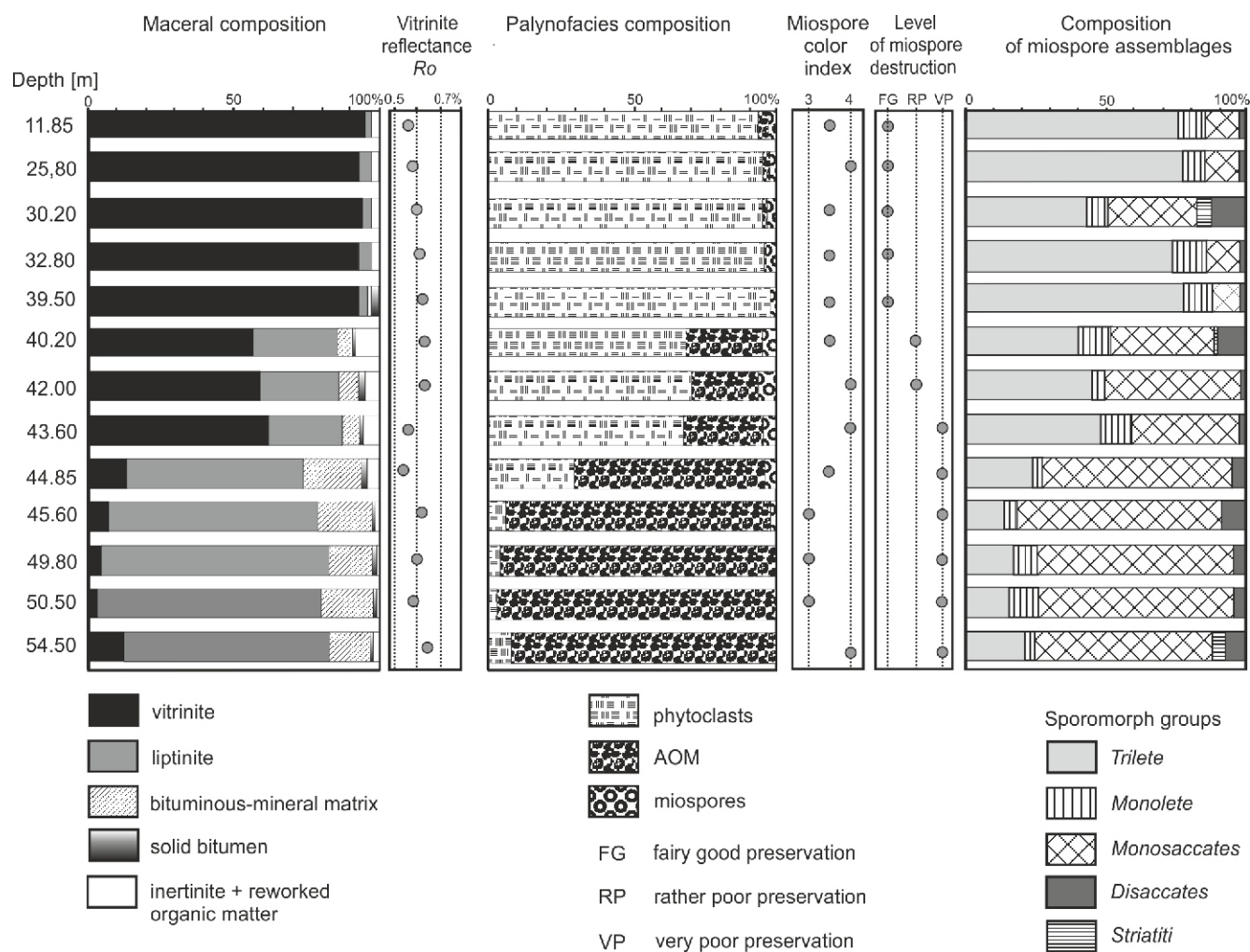
**Fig. 5. Organic petrography and vitrinite reflectance vs. palynofacies of the Ścinawka Średnia PIG 1 borehole**

content, mainly of *Monosaccites* but also *Disaccites,* is observed upwards in both profiles (Figs. 4 and 5).

ROCK-EVAL PYROLYSIS

Selected samples were analyzed by Rock-Eval pyrolysis to identify kerogen type and determine maturity level as well as to evaluate the general potential for hydrocarbon generation in the Anthracosia Shales in both the boreholes. The Rock-Eval analysis revealed that the amount of free hydrocarbons (S1 parameter) thermally liberated from a rock sample at 300°C is in the range of 0.02–0.59 mg HC/g rock (Table 5). Hydrocarbons released from a rock sample at a temperature range of 300–650°C (S2 parameter – also called the generative potential) fluctuate in a wide range of values between 0.04 and 10.8 mg HC/g rock. The $T_{max}$ temperature measured at the top of the S2 pyrolysis curve ranges between 439 and 461°C. The HI (also called the hydrocarbon potential) and OI indices are in a very wide range of values, of 20–375 mg HC/g TOC and 3–146 mg $CO_2$/g TOC, respectively. The TOC content is characterized by both lower and higher values, from 0.05 wt.% to 2.9 wt.%. The content of pyrolyzable carbon (PC) falls in a range between 0.01 and 0.94 wt.%, while the content of residual carbon (RC) oscillates between 0.04 and 1.93 wt.%. The sum of the PC and RC gives the TOC values. The Mineral Carbon

Content (MinC) varies from 0.05 to 5.4%, which may reflect the 0.4-43.3% carbonate content in the rocks samples analysed. In turn, the values of the production index (PI) range from 0.04 to 0.22.

DISCUSSION

ORGANIC ASSOCIATIONS

Results of the maceral quantitative analyses show the predominance of macerals of both vitrinite and liptinite groups in most of the samples, whereas those of the inertinite group are rare. Based on the organic matter composition, the Anthracosia Shales are classified into the following associations that have been distinguished based on the terminology proposed by Nowak (2007), and their detailed characteristics are additionally described using features of the palynofacies:

1. Bituminous association[1] (BA) – this is based on bituminite abundance in maceral composition. In general, bituminite is considered a byproduct of complete decomposition of various organic progenitors, e.g., algae, animal plankton, bacterial lipids (Teichmüller and Ottenjann, 1977; Robert, 1979; Stach et al., 1982; Taylor et al., 1998; Kus et al., 2017; Pickel et al., 2017; Liu et

---

[1] A former name lacustrine sapropelic association (Nowak, 2007) was more connected to the depositional environment of the shales examined. However, the name bituminous association as currently applied, is closely connected to the general term "organic association", where the adjective bituminous, similarly as the adjective humic used in the name "humic association", more closely reflects the type of organic matter (based on composition) occurring in the specific organic-mineral association

Table 5

**Rock-Eval pyrolysis data of samples of the Anthracosia Shales from the Intrasudetic Basin**

| No. | Borehole | Depth [m] | S1 [mg HC/ g Rock] | S2 [mg HC/ g Rock] | $T_{max}$ [°C] | HI [mg HC/ g TOC] | OI [mg CO$_2$/ g TOC] | PI | TOC [wt.%] | RC [wt.%] | PC [wt.%] | MinC [%] |
|---|---|---|---|---|---|---|---|---|---|---|---|---|
| 1 | Rybnica Leśna PIG 1 | 108.35 | 0.07 | 0.89 | 445 | 83 | 41 | | 1.07 | 0.94 | 0.14 | 0.82 |
| 2 | Rybnica Leśna PIG 1 | 113.20 | 0.04 | 0.10 | | 20 | 16 | | 0.48 | 0.45 | 0.03 | 0.34 |
| 3 | Rybnica Leśna PIG 1 | 119.50 | 0.03 | 0.06 | | 33 | 25 | | 0.18 | 0.17 | 0.01 | 0.10 |
| 4 | Rybnica Leśna PIG 1 | 132.70 | 0.06 | 0.93 | 445 | 80 | 10 | | 1.16 | 1.07 | 0.09 | 0.23 |
| 5 | Rybnica Leśna PIG 1 | 134.60 | 0.04 | 0.77 | 444 | 70 | 45 | | 1.10 | 1.00 | 0.10 | 0.47 |
| 6 | Rybnica Leśna PIG 1 | 137.70 | 0.11 | 0.89 | 447 | 91 | 8 | 0.11 | 0.99 | 0.90 | 0.09 | 0.20 |
| 7 | Rybnica Leśna PIG 1 | 139.90 | 0.32 | 2.8 | 445 | 175 | 4 | 0.10 | 1.62 | 1.35 | 0.27 | 0.31 |
| 8 | Rybnica Leśna PIG 1 | 140.25 | 0.07 | 0.70 | 446 | 70 | 12 | | 1.00 | 0.93 | 0.07 | 0.19 |
| 9 | Rybnica Leśna PIG 1 | 141.90 | 0.53 | 7.6 | 449 | 304 | 4 | 0.07 | 2.5 | 1.82 | 0.68 | 2.4 |
| 10 | Rybnica Leśna PIG 1 | 142.85 | 0.12 | 0.52 | 446 | 100 | 11 | 0.19 | 0.52 | 0.47 | 0.06 | 0.63 |
| 11 | Rybnica Leśna PIG 1 | 143.90 | 0.49 | 6.2 | 447 | 292 | 3 | 0.07 | 2.1 | 1.57 | 0.56 | 4.3 |
| 12 | Rybnica Leśna PIG 1 | 144.20 | 0.59 | 7.0 | 444 | 309 | 3 | 0.08 | 2.3 | 1.62 | 0.63 | 2.1 |
| 13 | Rybnica Leśna PIG 1 | 150.60 | 0.05 | 0.13 | | 62 | 9 | | 0.21 | 0.19 | 0.02 | 0.15 |
| 14 | Rybnica Leśna PIG 1 | 154.80 | 0.03 | 0.08 | | | | | 0.05 | 0.04 | 0.01 | 0.86 |
| 15 | Rybnica Leśna PIG 1 | 166.70 | 0.03 | 0.05 | | | | | 0.09 | 0.09 | 0.01 | 0.62 |
| 16 | Rybnica Leśna PIG 1 | 179.20 | 0.02 | 0.06 | | 22 | 28 | | 0.26 | 0.25 | 0.01 | 0.34 |
| 17 | Ścinawka Średnia PIG 1 | 11.85 | 0.03 | 0.11 | | 30 | 68 | | 0.37 | 0.35 | 0.02 | 0.05 |
| 18 | Ścinawka Średnia PIG 1 | 25.80 | 0.09 | 0.65 | 447 | 48 | 15 | | 1.36 | 1.29 | 0.07 | 0.19 |
| 19 | Ścinawka Średnia PIG 1 | 40.20 | 0.15 | 0.84 | 443 | 60 | 21 | 0.15 | 1.40 | 1.31 | 0.09 | 1.13 |
| 20 | Ścinawka Średnia PIG 1 | 42.00 | 0.17 | 1.16 | 443 | 106 | 15 | 0.13 | 1.09 | 0.98 | 0.12 | 1.28 |
| 21 | Ścinawka Średnia PIG 1 | 43.60 | 0.33 | 2.5 | 444 | 126 | 4 | 0.12 | 2.0 | 1.77 | 0.25 | 0.93 |
| 22 | Ścinawka Średnia PIG 1 | 44.85 | 0.25 | 0.89 | 443 | 92 | 23 | 0.22 | 0.97 | 0.87 | 0.10 | 0.99 |
| 23 | Ścinawka Średnia PIG 1 | 45.60 | 0.44 | 3.9 | 441 | 245 | 10 | 0.10 | 1.60 | 1.23 | 0.37 | 3.0 |
| 24 | Ścinawka Średnia PIG 1 | 49.80 | 0.32 | 8.8 | 440 | 367 | 5 | 0.04 | 2.4 | 1.63 | 0.76 | 4.9 |
| 25 | Ścinawka Średnia PIG 1 | 50.50 | 0.46 | 10.8 | 445 | 375 | 4 | 0.04 | 2.87 | 1.93 | 0.94 | 5.4 |
| 26 | Ścinawka Średnia PIG 1 | 54.50 | 0.02 | 0.04 | | | | | 0.10 | 0.09 | 0.01 | 2.1 |
| 27 | Ścinawka Średnia PIG 1 | 57.50 | 0.03 | 0.07 | | 49 | 102 | | 0.15 | 0.13 | 0.01 | 1.53 |
| 28 | Ścinawka Średnia PIG 1 | 60.00 | 0.02 | 0.05 | | 39 | 146 | | 0.12 | 0.11 | 0.01 | 2.3 |
| 29 | Ścinawka Średnia PIG 1 | 62.50 | 0.03 | 0.14 | | 46 | 62 | | 0.30 | 0.28 | 0.02 | 3.3 |
| 30 | Ścinawka Średnia PIG 1 | 63.75 | 0.03 | 0.07 | | 47 | 62 | | 0.14 | 0.13 | 0.01 | 1.05 |

S1 – the amount of free hydrocarbons liberated from a rock at 300°C; S2 – the hydrocarbons released from a rock between 300 and 650°C; $T_{max}$ – maximum temperature of the S2 peak; HI – hydrogen index; OI – oxygen index; PI – production index; TOC – total organic carbon content; RC – residual carbon content; PC – pyrolyzable carbon content; MinC – mineral carbon content

al., 2017). A typical feature of bituminite is the lack of a specific or distinct form. Alginite, present in much lesser quantities, occurs as both lamellae of lamalginite and telaginite (terminology commonly used in the liptinite classification of Cook et al., 1982, Taylor et al., 1998; Pickel et al., 2017; Kus et al., 2017). Both these types of alginite differ from each other not only in size and morphology, but also in fluorescence character, which is an important optical feature of alginite. Telaginite shows slightly brighter fluorescence compared to lamalginite. However, the alginite fluorescence is relatively intense and stronger than that of sporinite from the same samples. In this association, "dark vitrinite", solid bitumens, liptodetrinite and bituminous-mineral matrix (BMM) have been also encountered. Sporinite may also appear sporadically. Bituminite is also the main organic component of BMM, that is the background for the other lipid constituents listed herein. Therefore, BMM is also a component of the bituminous association. BMM may be compared to mineral-bituminous groundmass (Teichmüller and Ottenjann, 1977) or matrix-bituminite (Creaney, 1980). In the previous papers on OM petrography of the Anthracosia Shales (Nowak, 2003, 2007), this kind of mineral-organic material was referred to as the mineral-sapropelic matrix. However, in this paper we recommend the term bituminous-mineral matrix. (BMM) as more appropriate. Mixtures of bituminite, alginite, and liptodetrinite, along with solid bitumens, form an organic component of this material (Fig. 3G). Mineral-bituminous groundmass is widely distributed where mudstones are the source rocks. This kind of groundmass is the main hydrocarbon constituent of source rocks having a similar hydrocarbon generation potential to bituminite (Taylor et. al., 1998). "Dark vitrinite", occurring in some of the samples studied, is attributed to a sapropelic environment (ICCP, 1998). As noted above, secondarily altered organic matter has been observed in the shales under study. Mastalerz et al. (2018) indicate its reflectance as the petrographic criterion defining this type of OM. They distinguished two
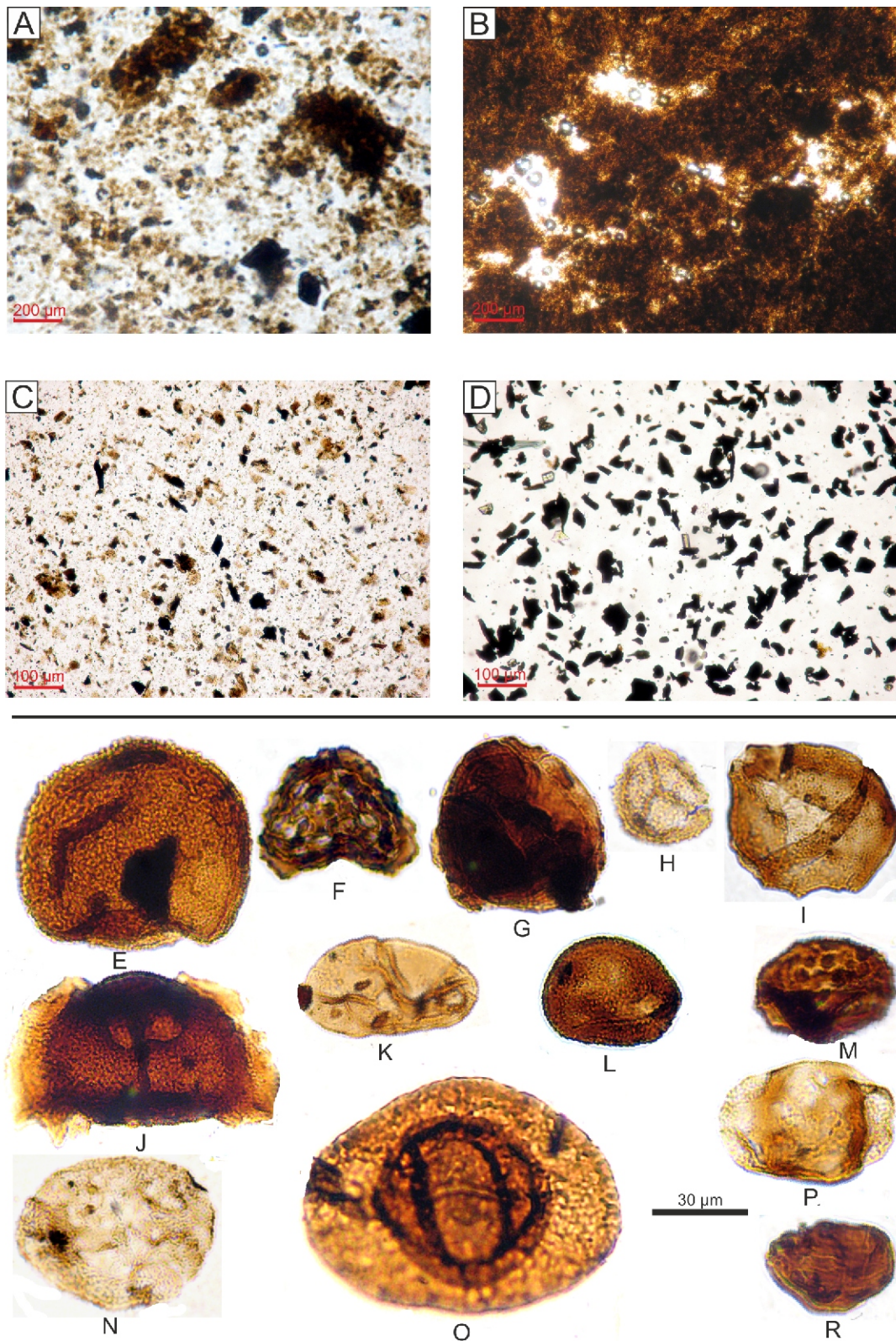
**Fig. 6. Palynofacies and miospores of the Anthracosia Shales**

**A** – palynofacies with very abundant AOM and sparse phytoclasts, Rybnica Leśna PIG 1 borehole, depth 142.85 m; **B** – palynofacies with very abundant AOM and sparse phytoclasts, Rybnica Leśna PIG 1 borehole, depth 143.9 m; **C** – palynofacies with abundant AOM and numerous phytoclasts, Ścinawka Średnia PIG 1 borehole, depth 44.85 m; **D** – palynofacies consisting of very numerous phytoclasts, Rybnica Leśna PIG 1 borehole, depth 121.8 m; **E** – *Verrucosisporites microtuberosus*, Rybnica Leśna PIG 1 borehole, depth 132.7 m; **F** – *Savitrisporites camptotus*, Rybnica Lśna PIG 1 borehole, depth 139.9 m; **G** – *Angulisporites splendidus*, Rybnica Leśna PIG 1 borehole, depth 140.25 m; **H** – *Lycospora pusilla*, Rybnica Leśna PIG 1 borehole, depth 132.7 m; **I** – *Crassispora kosankei*, Rybnica Leśna PIG borehole, depth 141.9 m; **J** – *Cirratriradites saturni*, Ścinawka Średnia PIG 1 borehole, depth 11.85 m; **K** – *Laevigatosporites vulgaris*, Rybnica Leśna PIG 1 borehole, depth 140.25 m; **L** – *Spinosporites spinosus*, Rybnica Leśna PIG 1 borehole, depth 132.7 m; **M** – *Thymospora* sp., Ścinawka Średnia PIG 1 borehole, depth 43.6 m; **N** – *Florinites pumicosus*, Ścinawka Średnia PIG 1 borehole, depth 44.85 m; **O** – *Potonieisporites novicus*, Ścinawka Średnia PIG 1 borehole, depth 44.85 m; **P** – *Limitisporites* sp., Rybnica Leśna PIG 1 borehole, depth 139.9 m; **R** – *Vittatina costabilis*, Ścinawka Średnia PIG 1 borehole, depth 44.85

types of this material. The first is solid bitumen, while the second is pyrobitumen. The boundary between these two types is set at a reflectance of 1.50% measured on solid bitumen ($B_{Ro}$) for bitumen (or 1.3% for sulfur-rich kerogens). The new classification of bitumen (Sanei, 2020) proposes (as in the above-cited article by Mastalerz et al., 2018) a division into solid bitumen and pyrobitumen. Solid bitumen occurs in rocks of $V_{Ro}$ <1.4%, while pyrobitumen occurs in rocks of $V_{Ro}$ >1.4%. Taking into account the thermal maturation level determined by the values of $V_{Ro}$ (Lewan, 1983), the solid bitumen occurring in the shales under study is associated with the initial stage of oil generation ($V_{Ro}$ ~ 0.5–0.7%). The solid bitumen content of the Anthracosia Shale is negligible, nevertheless the solid bitumen content of lacustrine shales can locally be significant and these components can be predominant in organic matter composition (Hackley et al., 2017; Guo et al., 2018). Optically, the bituminous association is characterized by more or less intense fluorescence visible during UV irradiation. Fluorescence intensity depends on more than the bituminous material prevailing in the sample. The bituminite-predominant samples show a relatively weak intensity of fluorescence; however, it changes to more intense when alginite, liptodetrinite or solid bitumens and sporinite occur in the petrographic composition. This association is determinable only in UV irradiation. The high-fluorescence shales in this study suggest that the organic matter has either a high hydrogen index or an enhanced lipid content. The palynofacies of this association is dominated by amorphous organic matter. Phytoclasts are rather abundant and sporomorphs are few. In the sporomorph assemblage, the *Monosaccites* group is the most abundant and remaining groups are less numerous. The shales of this association are present in both the boreholes studied. In the profile of the Rybnica Leśna PIG 1 borehole, rocks of this association were identified in the depth interval 141.9–143.9 m, while in the profile of the Ścinawka Średnia PIG 1 borehole shales of this association occur in the depth interval 44.85–54.5 m.

2. Humic association (HA) – this is defined for shales characterized by a relatively high content of coaly humic particles of terrestrial origin. This type contains mainly vitrinite with a lesser inertinite contribution and liptinite (sporinite and liptodetrinite). Macerals of both the vitrinite and inertinite groups are easily recognizable in white light. Only sporinite and liptodetrinite show yellow fluorescence visible during UV irradiation. The palynofacies of this association is dominated by phytoclasts with a small content of fairy well-preserved sporomorphs. The sporomorphs of the *Triletes* group are the most abundant, and the *Monoletes* group is a constant component present in smaller numbers. The frequency of sporomorphs from the *Monosaccites* group is low in the Rybnica Leśna PIG 1 profile and significantly higher in the Ścianawka Średnia PIG 1 profile. The *Disaccites* group occurs in small numbers, slightly higher in the latter profile (Figs. 5 and 6). The shales of this association occur in the depth intervals 108.35–125.50 m and 11.85–39.50 m in the Rybnica Leśna PIG 1 and Ścinawka Średnia PIG 1 boreholes, respectively.

3. Intermediate association (IA) – this association contains organic components of both associations distinguished above. The organic matter composition of this association can show predominance of either humic or bituminous material. The palynofacies are dominated by phytoclasts, but AOM also occurs and is a stable and important component. The sporomorph assemblage shows an intermediate composition with the *Triletes* and *Monosaccites* groups in similar proportions (Figs. 4 and 5). Shales with this association are clearly evident in the profile of the Ścinawka Średnia PIG 1 borehole only, in the depth interval 40.2–43.6 m (Fig. 5). In the profile of the Rybnica Leśna PIG 1 borehole it is possible to recognize them taking into account the combined content of liptinite, BMM and/or solid bitumens which is higher than the content of these components in humic association. In this borehole the shales of the intermediate association are of strongly humic character with transitions to shales of the humic association. In this borehole the shales of with the intermediate association occur in the 132.70–140.25 m depth interval (Fig. 4).

The contents of vitrinite, liptinite and inertinite and other organic matter components are illustrated in Figure 7. The above associations were identified in the maceral composition of rocks studied from the Rybnica Leśna PIG 1 and Ścinawka Średnia PIG 1 boreholes. Samples from the Rybnica Leśna PIG 1 borehole are grouped within two areas of the diagram (Fig. 7). The first is located near the vitrinite vertex, and indicates that the samples belong to either the humic or intermediate (of humic character) associations. In contrast, samples of the second concentration area in the diagram occur adjacent to the liptinite + BMM + SB apex, showing the bituminous association of these samples. The position of the intermediate association, though,
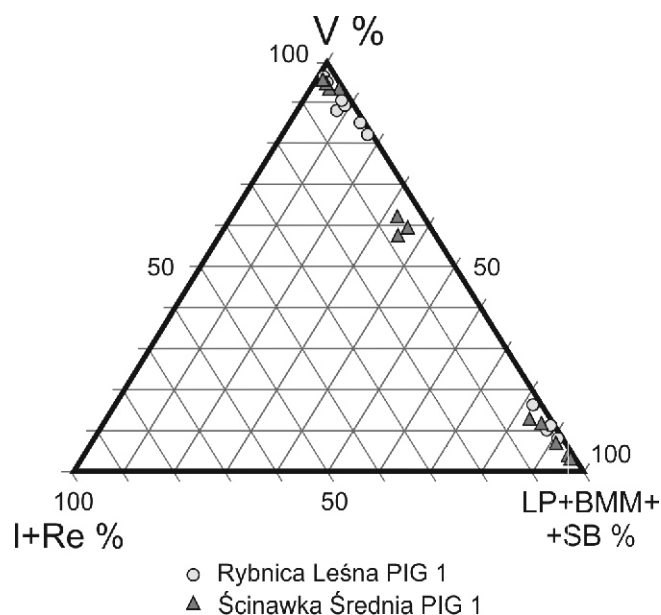


**Fig. 7. Ternary plot of vitrinite–liptinite + bituminous mineral matrix + solid bitumen–inertinite + recycled vitrinite of the Anthracosia Shales samples of the Rybnica Leśna PIG 1 and Ścinawka Średnia PIG 1 boreholes**

V – vitrinite, LP – liptinite, BMM – bituminous-mineral matrix, SB – solid bitumen, I – inertinite, RE – recycled vitrinite

is not so clearly visible as that observed in the shales of the Ścinawka Średnia PIG 1 borehole (Fig. 7). In the Ścinawka Średnia PIG 1 borehole, three associations occur. Samples in which the humic association dominates are located in the immediate vicinity of the vitrinite apex. Samples with a dominance of the bituminous association occur directly near the apex of the liptinite + BMM + SB components, while samples in which the intermediate association occurs are located between the vitrinite – and liptinite + BMM + SB vertices.

## DEPOSITIONAL ENVIRONMENT

The geological, sedimentological and organic petrographic data indicate that the Anthracosia Shales were deposited in a lacustrine environment (Dziedzic, 1959, 1961; Mastalerz and Wojewoda, 1988; Mastalerz and Nehyba, 1997; Nowak, 2007). A typical feature of the Carboniferous-Permian lacustrine shales of Central Europe is their visible lamination (Mastalerz, 1990; Mastalerz and Nehyba, 1997; Martinek et al., 2006; Lojka et al., 2010), as in the Anthracosia Shales described here, as well as in Nowak (2007). These shales are naturally divided into two types according to different kinds of lamination. One of these is related to the finest-grained lithology and is dark grey or black. It is enriched in bituminite with alginite and BMM. These components are fluorescencent. The presence of laminae enriched in microscopically visible organic matter is a sedimentary record of the high bio-productivity of lacustrine environments (Zang et al., 2017). The second type forms thicker clay-rich laminae with a little bituminite, while vitrinite with a small content of inertinite and sporinite is much more frequent. These kinds of laminae are associated with cooler and drier periods of lake development with lower bio-productivity of bituminous material and a predominance of terrigenous organic matter. However, the thinner and darker laminae, which consist mainly of lipid components, may be considered as having originated in warmer or more humid periods characterized by higher bio-productivity. They represent both bituminous and intermediate associations. The lamination of the shales may be related to seasonal changes during their sedimentation, typical of stratified lakes. The Anthracosia Lake was of this type (Mastalerz and Nehyba, 1997).

Organic material dispersed in the Anthracosia Shales is derived from various sources, such as lipid-enriched phytoplankton and terrigenous humic OM. Organic petrography and palynology classified the Anthracosia Shales into three associations recognized here on the basis of their maceral and palynofacies compositions. The bituminous association is associated with a deeper (open-water) part of the Anthracosia Lake, a bituminite and BMM environment where alginite also occurs. The latter is represented chiefly by lamalginite with a lower proportion of telalginite and some wind-blown sporinite. The marginal and lake basin areas also differ significantly in both the composition and distribution of organic matter. Liptinite macerals of aquatic origin, i.e., the lacustrine algal material, especially bituminite, prevail over terrestrial material in the bituminous association. The presence of alginite especially lamalginite, can suggest deposition in anoxic and stratified conditions, as is supported by the lack of burrowing infauna in these types of rocks (Demaison and Moore, 1980; Liu et al., 2017). Bituminite is a product of bacterial degradation of primary biomass consisting of algae, bacterial lipids, degraded animal plankton and other precursors (Teichmüller, 1974; Robl et al., 1992; Obermajer et al., 1997; Taylor et al., 1998; Rimmer et al., 2004; Kus et al., 2017; Pickel et al., 2017). The high content of bituminite and bituminous-mineral matrix in combination with the very fine pyrite replacing organic particles (alginite and sporinite), indicates the prevailing reducing conditions, where authigenesis of sulfide minerals took place. These conditions favoured transformation of alginite and the rest of the biomass material into bituminite. Similar relationships have been noted in Stephanian lacustrine shales in the central and western parts of the Bohemian Basins (Lojka et al., 2010). The prevalence of bituminite and BMM over alginite in the OM composition indicates conditions favourable for advanced processes of algal decomposition and bituminite formation. Such conditions favoured the replacement of alginite by bituminite. This phenomenon has been observed during previous studies of the Anthracosia Shales (Nowak, 2003, 2007). The dominant components of the bituminous association of both boreholes are bituminite, with smaller contents of BMM and alginite. However, in the previously examined shales from both the Ścinawka Dolna IG 1 and the Bożków IG 1 boreholes, an equivalent of the bituminous association was called the lacustrine sapropelic association and was divided into two types (Nowak, 2007). One of these is characterized by the presence of predominant alginite and associated with autochthonous subaqueous sedimentation. In the second type, bituminite is the dominant component, while alginite occurs as single lamellae of lamalginite. The equivalent of the latter type of lacustrine sapropelic association is present in both the Ścinawka Średnia PIG 1 and Rybnica Leśna PIG 1 boreholes and is here called the bituminous association. The results of the maceral analysis indicate the dominance of bituminite and other lipid components of this association. Also, the palynofacies analysis pointed to AOM as the main component of the bituminous association. In places phytoclasts also accompany AOM (Figs. 4 and 5). Palynological results show that sporomorphs in this association are pollen grains, which were wind-transported. The *Monosaccites* group are usually more numerous than others in both profiles and the *Disaccites* and *Striatiti* groups slightly more frequent in the Ścinawka Średnia borehole. A similar miospore assemblage from Triassic deposits has been interpreted as distal lacustrine (Fijałkowska-Mader at al., 2015). The reducing conditions in which this association was formed was a factor in the poor preservation of the miospores. Based on the Rock-Eval data, the deep-water shales studied represent mainly type I kerogen. Taking into account all the maturity parameters, the deep-water shales are thermally early-mature.

The humic association contains mostly terrestrial macerals like vitrinite (the most abundant), sporinite, and negligible inertinite. They are recognized as plant remnants of the immediate surroundings of the Anthracosia Lake, which were deposited in a coastal zone of lower water table. Most of the terrigenous organic matter did not experience long-distance aquatic transport. Macerals occurring in the humic association are characterized by a relatively good state of preservation, as are phytoclasts and miospores of the association. Vitrinite in shales of the coastal zone may locally show a granular surface due to hydrocarbon leaching. Larger inertinite fragments show cellular morphology, which may be interpreted as reflecting deposition near the source area. The very light grey colour of inertinite in comparison to the grey and dark grey colour of vitrinite indicates that the inertinite has the highest reflectance of all the macerals in the association. This feature of inertinite is connected to its genesis, pointing to a high-temperature origin, most probably generated by wildfires (Scott and Jones, 1994; Uglik and Nowak, 2015; Liu et al., 2018; Scott, 2020, 2022). The results of palynofacies analysis indicate that phytoclasts are most numerous in rocks of this association. The results also revealed the scarcity of amorphous organic matter in the rocks with the HA, while the organic petrographic data do not record the presence of such material, referred to as bituminite in

petrographic research. The miospore assemblages from the samples containing the humic association are dominated by sporomorphs produced by sphenopsids and ferns, belonging to the *Triletes* and *Monoletes* groups. The *Triletes* group dominates in rocks of this association in both profiles, while the *Monoletes* group is less abundant. The *Monoletes* group is more generally abundant in samples from the Rybnica Leśna PIG 1 profile compared to the Ścinawka Średnia PIG 1 profile. Organic matter, which was the precursor of vitrinite and inertinite, was probably produced by plants growing out of the lake, mainly ferns and sphenopsids. It was transported by rivers flowing into the lake and later distributed by lake currents. These components represent terrigenous organic matter in the shales. The terrestrial origin of this organic matter is demonstrated not only by the petrographic and palynofacies data, but also by the results of pyrolysis analysis in which type III kerogen was recognized in rocks of this OM composition. Type III kerogen comes predominantly from material of higher plants. Type III tends to be more gas-prone than other kerogen types, and is chemically analogous to the humic coal maceral represented chiefly by vitrinite. All parameters applied ($V_{Ro}$, $T_{max}$ and miospore colour index) indicate the early mature and mature stages of thermal maturity for rocks of this association.

The Anthracosia Shales from the previously studied Ścinawka Dolna IG 1 and Bożków IG 1 boreholes show a more uniform distribution of associations and a clear dominance of the bituminous type (Nowak, 2007) compared to data from the Ścinawka Średnia PIG 1 and Rybnica Leśna PIG 1 boreholes. Differences in the association distribution in particular shale units of the boreholes analysed correspond to different developmental phases of the Anthracosia Lake during the sedimentation of the rocks under study.

The existence of the Anthracosia Lake under the conditions of a warm and dry climate may be explained by a local change to much more humid conditions, in which local lakes could exist, which was favourable for the development of terrestrial vegetation. This concept is supported by thin coal intercalations within the Anthracosia Shales and the grey colour of the overlying sedimentary rocks of fluvial origin (Dziedzic, 1959, 1961). Formation of the Anthracosia Shales and the younger Walchia Shales and grey deposits among the red-brownish deposits is related to the occurrence of a protected reducing environment under the conditions of a warm and dry climate, as is the case of Lake Rudolph in Africa (Nowak, 2007).

### THERMAL MATURITY

As sampling was concentrated on potential source rocks, an important indicator for such rocks is the thermal maturity of the dispersed organic matter. The maturity of OM is evaluated based on vitrinite reflectance, palynomorph colour index and the maximum temperature. Results for the Anthracosia Shales samples show that vitrinite reflectance measurements generally display rather stable $VR_o$ values in both boreholes (Tables 1, 2 and Figs. 4, 5 ). Vitrinite reflectance values range from 0.53 to 0.65% and from 0.53 to 0.73% for shales from the Ścinawka Średnia PIG 1 and Rybnica Leśna PIG 2 boreholes, respectively. These values indicate that the organic matter is marginally to early mature (Dow, 1977; Peters and Cassa, 1994).

The palynofacies analyses show that the colour of the miospore specimens varies from yellow to orange-brown. The thermal maturation index based on *Lycospora* colours was assessed as 3–4 in the seven-level scale of Batten (1982, 1996). These values of miospore colour index indicate early mature to mature stages of OM thermal maturity. These data clearly correlate with the measured vitrinite reflectance (Figs. 4 and 5).

For most samples, $T_{max}$ – based OM maturity is in close agreement with results based on vitrinite reflectance. The $T_{max}$ values support the presence of early mature and mature organic matter with respect to hydrocarbon generation, which corresponds to oil window maturity (Table 5). Average $T_{max}$ values, which fluctuate in a very narrow range of 441–443°C, are typical for the middle oil window zone.
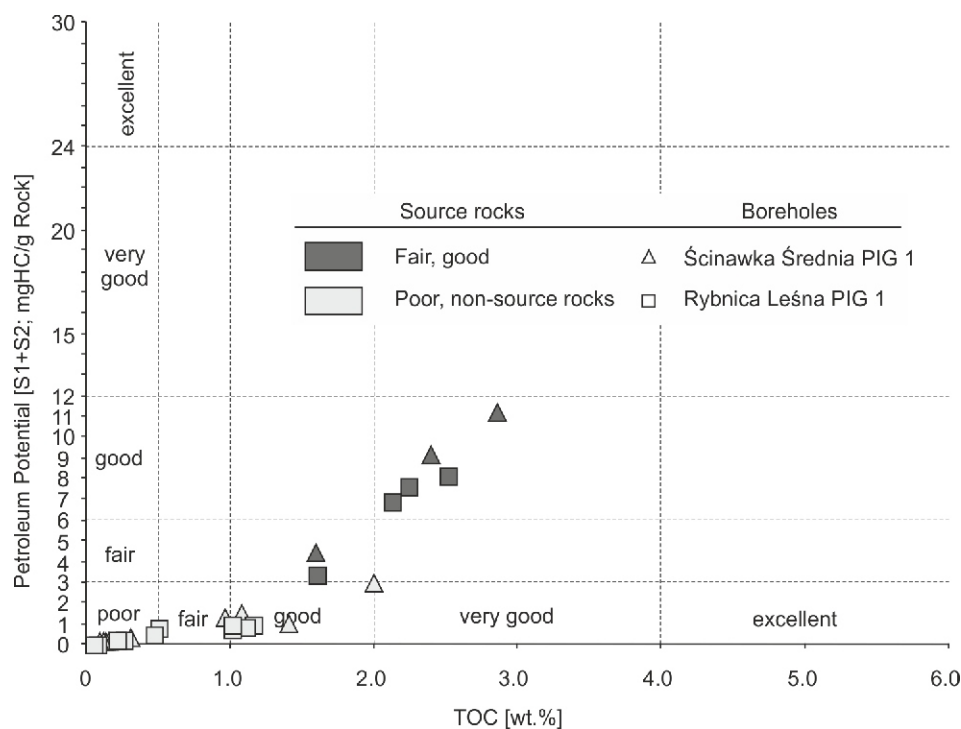


**Fig. 8. General classification of the source rock quality, bringing additional information concerning the petroleum potential of the Anthracosia Shales samples studied**

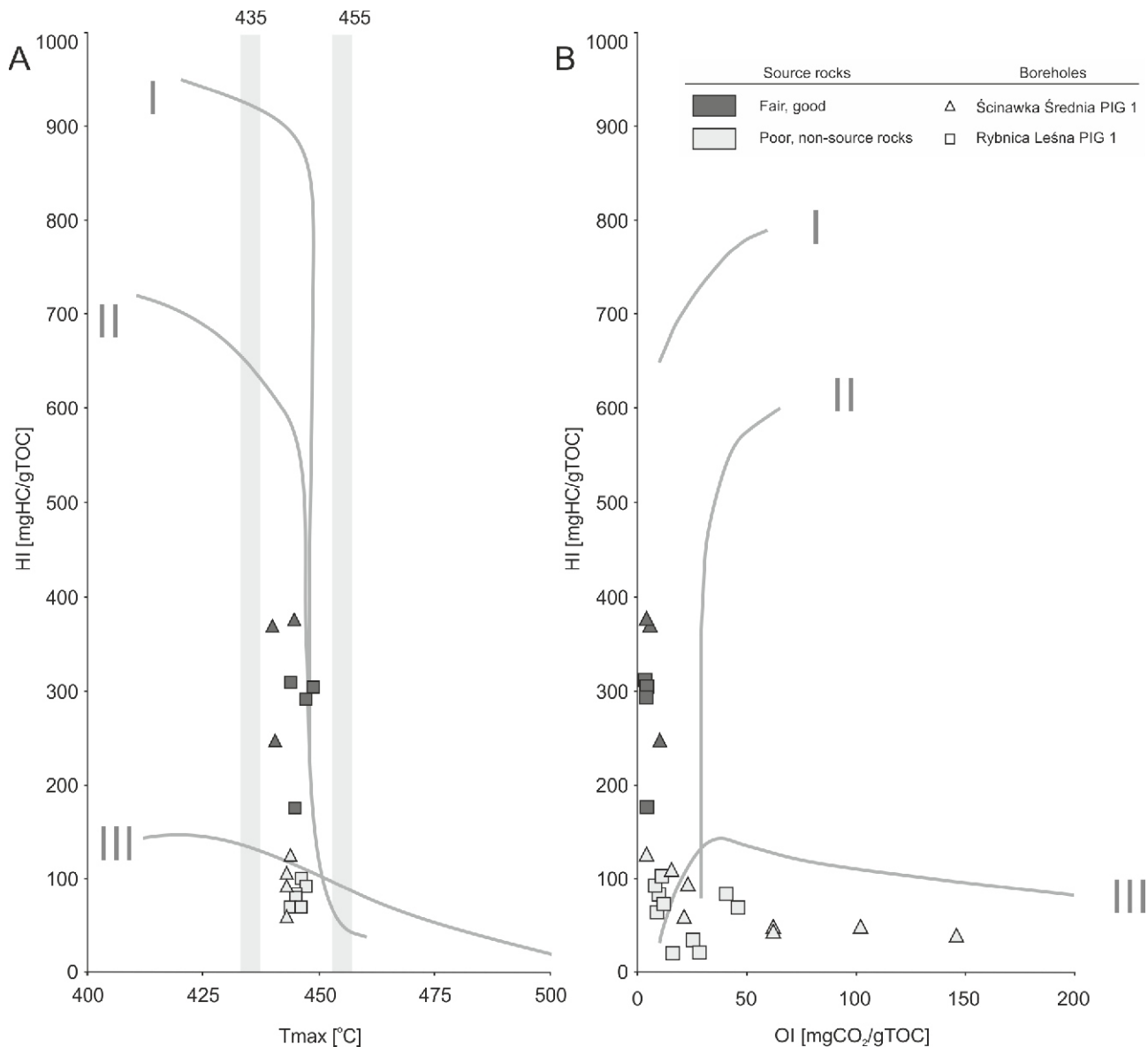PP    3 mgHC/gRock indicates rocks with good petroleum potential (Peters and Cassa, 1994)

**Fig. 9A** – correlation of HI–$T_{max}$ of the Anthracosia Shales samples shows type I kerogen, type III kerogen and hydrogen-depleted type III kerogen in early-mature and mature stages of organic matter maturity (after Espitalié et al., 1977); **B** – the HI–OI graph of the Anthracosia Shales samples shows a distinction between kerogen types and geochemically altered and oxidized samples from the Ścinawka Średnia PIG 1 borehole (after Pratt, 1984)

There were no significant changes in the values of individual maturity parameters in the vertical profiles of the shales studied.

### SOURCE ROCK POTENTIAL

Rock-Eval analysis revealed a lack of meaningful geochemical differences between the Rybnica Leśna PIG 1 and Ścinawka Średnia PIG 1 boreholes. Consequently, all the data may be described together.

The samples can be grouped simply, namely, (1) fair and good source rocks with S1 + S2 parameters ≥3 mg HC/g rock, and (2) poor and non-source rocks with (S1 + S2) <3 mg HC/g rock (Fig. 8). The division is also clearly seen on the HI/Tmax and HI/OI graphs (Fig. 9A, B) where hydrogen index values separate fair and good source rock samples (HI ≥175 mg HC/g TOC) from poor source rocks. Among the Anthracosia Shales samples, the fair and good source rocks are dominated by HI

values falling in a range between 175 and 375 mg HC/g TOC, while the poor and non-source rocks have HI values between 46 and 126 mg HC/g TOC. The samples represent early-mature and mature type I, and hydrogen-depleted type III kerogen. The latter group includes more oxidized samples especially in the Ścinawka Średnia PIG 1 borehole with OI ≥62 mg $CO_2$/g TOC (Table 5 and Fig. 9). However, the samples from the Ścinawka Średnia PIG 1 borehole with HI ≤49 mg HC / g TOC are clearly oxidized and are characterized by OI ≥62 mg $CO_2$ / g TOC. On the other hand, the MinC content of these samples is 0.05–3.3% and is lower than in the samples with type I (3.0–5.4% MinC) from the Ścinawka Średnia PIG 1 borehole.

The established zone of fair and good source rocks in the borehole section suggests that the good oil source rocks may be found in a narrow zone of the lower part of the Anthracosia Shales, between ~139.90 and ~144.20 m depth, forming a ~4.3 m thick unit in the Rybnica Leśna PIG 1 borehole. The unit
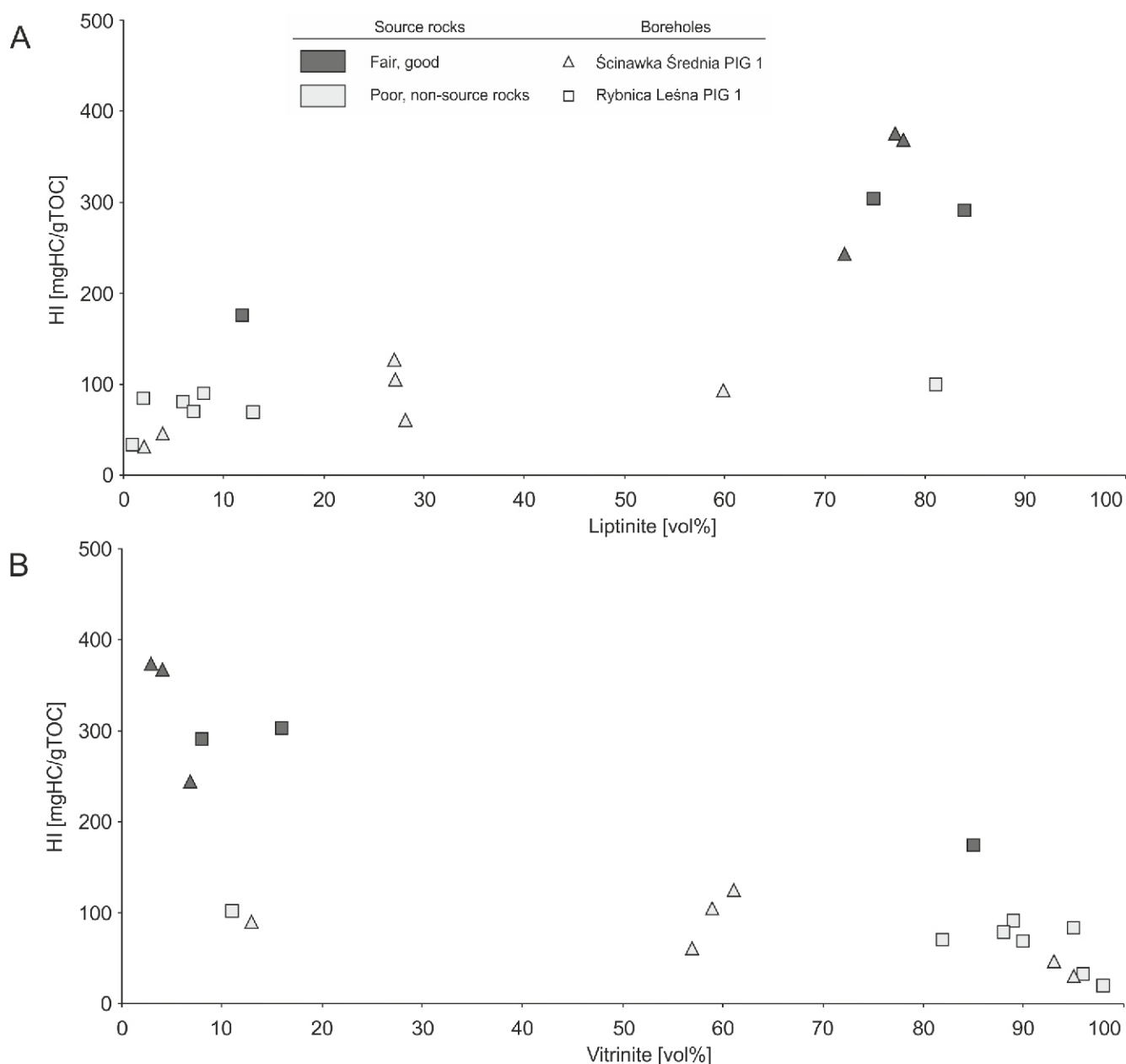
**Fig. 10. Correlation of the hydrogen index with the content of liptinite and vitrinite in samples from the Rybnica Leśna PIG 1 and Ścinawka Średnia PIG 1 boreholes**

of good source rocks in the Ścinawka Średnia PIG 1 borehole has a similar thickness of ~5 m, making up the middle part of the Anthracosia Shales profile between ~45.5 and ~50.5 m depth.

There is an interesting correlation of the kerogen types to the organic matter petrography results, where the contents of individual groups of macerals are described in great detail. In the Rybnica Leśna PIG 1 borehole, algal-originated kerogen is composed of a small amount of vitrinite (8–16 vol%) and a large amount of liptinite (75–84 vol.%), which explains the large amounts of bituminite detected (63–71 vol%) and higher values of the hydrogen index: 292–304 mg HC/g TOC (Fig. 10). In the terrigenous-originated kerogen, a rapid increase in the vitrinite content up to 82–98 vol% and a decrease in the liptinite content to 1–13 vol% was observed, which automatically converted into a decrease in the bitumen content and in hydrogen index values to 33–91 mg HC/g TOC. An analysis of the relationships

shows the following dependences: (i) the formation of fair to good source rocks depends on an abundant liptinite content, (ii) an increasing proportion of vitrinite significantly reduces the hydrogen content of the kerogen and the petroleum potential of the rocks. A similar relationship between the maceral composition and the values of the hydrogen index as well as the quality of the source rocks was noted in the Ścinawka Średnia PIG 1 borehole.

## CONCLUSIONS

The total thickness of the shales falls in the range of ~61–99 m. Organic petrography studies have shown a presence of different macerals dispersed in the Anthracosia Shales. Vitrinite and inertinite are particles of terrestrial origin, while most liptinite macerals are of aquatic provenance.

Organic petrography and palynofacies analysis of the Anthracosia Shales indicate the occurrence of three broadly distinct associations: (1) a bituminous association (which was deposited in a deepwater zone near the centre of the Anthracosia Lake); (2) a humic association, which was deposited in a coastal zone; (3) an intermediate association, which was deposited in a shallow zone of the Anthracosia Lake.

There are significant differences in the predominant type of organic association between the Rybnica Leśna PIG 1 and Ścinawka Średnia PIG 1 boreholes. In the former, a dominance of both the humic and intermediate (of humic character) associations is typical, with a lower participation of the bituminous association. However, in the Ścinawka Średnia PIG 1 borehole, the shales are characterized by predominance of both bituminous and intermediate associations, while the humic association occurs less frequently.

The changes in the composition of miospore assemblages in association with the variability of the maceral composition and geochemical parameters in both boreholes studied were interpreted as a record of the evolution of the lake in which the sedimentation took place. This clearly indicates that the composition of miospore assemblages cannot be used for stratigraphic purposes because it was very clearly controlled environmentally.

The results of the maceral analysis of the shales generally agree with data from both palynofacies and Rock-Eval pyrolysis studies. The dispersed organic matter does not demonstrate an unambiguously prominent character. The Rock-Eval data clearly indicate that the organic matter forms levels made up either of kerogen type I or of kerogen type III. Microscopic observations also show that the kerogen is relatively uniform in composition: (1) with bituminite (amorphous organic matter) abundant in type I kerogen and (2) with vitrinite, which predominates in type III kerogen. The results published here corroborate the previous results of earlier Anthracosia Shales studies (Nowak, 2007). These were based solely on organic petrography data and revealed a clear sapropelic character with a dominance of alginite in the organic matter composition of the Anthracosia Shales, indicative of type I source rocks.

The maturity parameters (vitrinite reflectance, miospore colour index, and Rock-Eval $T_{max}$) show an overall early-mature to mature stage for the Upper Carboniferous Anthracosia Shales in the Intrasudetic Basin. None of the maturity indicators show a consistent vertical trend.

The geochemical parameters obtained from the Rock-Eval pyrolysis of the samples indicate various petroleum potential, from poor to very good.The good source rocks (1.6–2.9 wt.% TOC, 3.2–10.8 mg HC/g rock – S2) are represented by only a ~4-5 m thick layer located in the lower and middle parts of the Rybnica Leśna PIG 1 and Ścinawka Średnia PIG 1 boreholes, respectively.

# REFERENCES

**Abou El-Anwar, E., Salman, S., Mousa, D., Aita, S., Makled, W., Gentzis, T., 2021.** Organic petrographic and geochemical evaluation of the black shale of the Duwi Formation, El Sebaiya, Nile Valley, Egypt. Minerals, **11**: 1416.

**Awdankiewicz, M., Kurowski, L., Mastalerz, K., Raczyński, P., 2003.** The Intra-Sudetic Basin – a record of sedimentary and volcanic processes in late- to postorogenic tectonic setting. Geolines, **16**: 165–183.

**Batten, D.J., 1982.** Palynofacies, palaeoenvironments and petroleum. Journal of Micropalaeontology, **1**: 107–114.

**Batten, D.J., 1996.** Palynofacies and petroleum potential. Palynology: principle and applications, **3**: 1065–1084. American Association of Stratigraphic Palynologists Foundation, Dallas.

**Bossowski, A., Ihnatowicz A., 1994.** Palaeogeography of the uppermost Carboniferous and lowermost Permian deposits in the NE part of the Intra-Sudetic Depression. Geological Quarterly, **38** (4): 709–726.

**Bossowski, A., Ihnatowicz, A., 2006.** Geological Atlas of the Lower Silesian Coal Basin 1:100 000. Polish Geological Institute, Warszawa.

**Bossowski, A., Ihnatowicz, A., Mastalerz, K., Kurowski, L., Nowak, G. 1995.** Lithostratigraphy and sedimentologic-paleogeographic development. Sudetes and Fore-Sudetic area. Intra-Sudetic Depression. Prace Państwego Instytutu Geologicznego, **148**: 142–147.

**Carroll, A.R., Brassell, S.C., Graham, S.A., 1992.** Upper Permian lacustrine oil shales, southern Junggar basin, northwest China. AAPG Bulletin, **76**: 1874–1902.

**Carvajal-Ortiz, H., Gentzis, T., 2018.** Geochemical screening of source rocks and reservoirs: the importance of using the proper analytical program. International Journal of Coal Geology, **190**: 56–69.

**Cook, A.C., Hutton, A.C., Sherwood, N.R., 1982.** Alginite nomenclature. Letter to MOD Commission of the International Committee for Coal Petrology, April 1982.

**Creaney S., 1980.** The organic petrology of the Upper Creataceous Boundary Creek formation, Beaufort-Mackenzie basin. Bulletin of Canadian Petroleum Geology, **28**: 112–119.

**Deaf, A.S., Tahoun, S., Gentzis, T., Carvajal-Ortiz, H., Harding, I.A., Marshall, J.E.A., Ocubalidet, S., 2020**. Organic geochemical, palynofacies, and petrographic analyses examining the hydrocarbon potential of the Kharita Formation (Albian) in the Matruh Basin, northwestern Egypt. Marine and Petroleum Geology, **112**: 104087.

**Demaison, G., Huizinga, B.J., 1991**. Genetic classification of petroleum systems. AAPG Bulletin, **75**: 1626–1643.

**Demaison, G.J., Moore, G.T., 1980.** Anoxic environments and oil source bed genesis. Organic Geochemistry, **2**: 9–31.

**Don, J., 1961.** The Permo-Carboniferous of the Nowa Ruda region (in Polish with English summary). Zeszyty Naukowe Uniwersytetu Wrocławskiego, Nauka o Ziemi, **3**: 3–49.

**Dow, W.G., 1977.** Kerogen studies and geological interpretations. Journal of Geochemical Exploration, **7**: 79–99.

**Dunn, M.T., 2001**. Palynology of the Carboniferous–Permian boundary stratotype, Aidaralash Creek, Kazakhstan. Review of Palaeobotany and Palynology, **116**: 175–194.

Dyni, J.R., 2006. Geology and resources of some world oil-shale deposits. U.S. Geological Survey Scientific Investigations Report, 2005-5294.

Dziedzic, K., 1959. Comparison of Rotliegendes sediments in the region of Nowa Ruda (Middle Sudetes) and Świerzawa (Western Sudetes) (in Polish with English summary). Geological Quarterly, 3: 831–846.

Dziedzic, K., 1961. Lower Permian in the Intrasudetic Basin (in Polish with English summary). Studia Geologica Polonica, 6: 1–124.

Espitalié, J., Madec, M., Tissot, J., Menning, J., Leplat, P., 1977. Source rock characterization method for petroleum exploration. Proceedings 9th Annual Offshore Technology Conference, 3: 439–448.

Fijałkowska-Mader, A., Kuleta, M., Zbroja, S., 2015. Lithostratigraphy, palynofacies and depositional environments of the Triassic deposits in the northern part of the Nida Basin (in Polish with English summary). Biuletyn Państwowego Instytutu Geologicznego, 462: 83–124.

Ghazwani, A., Littke, R., Sachse, V., Fink, R., Mahlstedt, N., Hartkopf-Fröder, C., 2019. Organic geochemistry, petrology and palynofacies of Middle Devonian lacustrine flagstones in the Orcadian Basin, Scotland: depositional environment, thermal history and petroleum generation potential. Geological Magazine, 155: 773–796.

Goodarzi, F., Gentzis, T., Sanei, H., Pedersen, P.K., 2019. Elemental composition and organic petrology of a Lower Carboniferous-age freshwater oil shale in Nova Scotia, Canada. ACS Omega, 4: 20773–20786.

Górecka, T, 1981. Results of plynological studies of the Youngest Carboniferous of the Lower Silesia (in Polish with English summary). Prace Naukowe Instytutu Górnictwa Politechniki Wrocławskiej, Monografie, 19: 1–58.

Górecka-Nowak, A., 1989. Late Carboniferous spore-pollen assemblages of the Unisław IG-1 borehole (in Polish with English summary). Prace Naukowe Instytutu Górnictwa Politechniki Wrocławskiej, 52, Studia i Materiały, 19: 51–57.

Górecka-Nowak, A, 1995. Palynostratigraphy of the Westphalian deposits of the nort-western part of the Intrasudetic Basin (in Polish with English summary). Acta Universitatis Wratislaviensis, Prace Geologiczno-Mineralogiczne, 40.

Górecka-Nowak, A., 2008. Palynostratigraphy of the up per most Carboniferous and lowermost Permian sediments in the Sudetes (SW Poland). Terra Nostra, 2: 97.

Górecka-Nowak, A., Nowak, G.J., 2008. Charakterystyka petrologiczna i palinologiczna materii organicznej czarnych łupków Sudetów (in Polish). In: First Polish Geological Congres, Kraków (ed. G. Haczewski), Abstracts: 32 .

Graham, S.A., Brassell, S., Carroll, A.R., Xiao, X., Demaison, G., Mcknight, C.L., Liang, Y.,Chu, J., Hendrix, M.S., 1990. Characteristics of selected petroleum source rocks, Xinjiang Uygur Autonomous Region, northwest China. AAPG Bulletin, 74: 493–512.

Guo, H., He, R., Jia, W., Peng, P., Lei,Y., Luo, X., Wang, X., Zhang, L Jiang, C., 2018. Pore characteristics of lacustrine shale within the oil window in the Upper Triassic Yanchang Formation, southeastern Ordos Basin, China. Internationonal Journal of Coal Geology, 91: 279–296.

Hackley, P.C., Cardott, B.J., 2016. Application of organic petrography in North American shale petroleum systems: a review. International Journal of Coal Geology, 163: 8–51.

Hackley, P.C., Araujo, C.V., Borrego, A.G., Bouzinos, A., Cardott, B.J., Cook, A.C., Eble, C., Flores, D., Gentzis, T., Gonçalves, P.A., Mendonça Filho, J.G., Hámor-Vidó, M., Jelonek, I., Kommeren, K., Knowles, W., Kus, J., Mastalerz, M., Menezes, T.R., Newman, J., Oikonomopoulos, I.K., Pawlewicz, M., Pickel, W., Potter, J., Ranasinghe, P., Read, H., Reyes, J., Rosa Rodriguez, G.D.L., Alves Fernandes de Souza, I.V., Suárez-Ruiz, I., Sýkorová, I., Valentine, B.J., 2015. Standardization of reflectance measurements in dispersed organic matter: results of an exercise to improve interlaboratory agreement. Marine and Petroleum Geology, 59: 22–34.

Hackley, P.C., Fishman, N., Wu, T., Baugher, G., 2016. Organic petrology and geochemistry of mudrocks from the lacustrine Lucaogou formation, Santanghu Basin, northwest China: application to lake basin evolution. International Journal of Coal Geology, 168: 20–34.

Hackley, P.C., Zhang, L., Zhang, T., 2017. Organic petrology of peak oil maturity Triassic Yanchang Formation lacustrine mudrocks, Ordos Basin, China. Interpretation, 5: SF211–SF223.

Huijuan, G., Ruliang, H., Wanglu, J., Ping'an, P., Yuhong, L., Xiaorong, L., Xiangzeng, W., Lixia, Z., Chengfu, J., 2018 Pore characteristics of lacustrine shale within the oil window in the Upper Triassic Yanchang Formation, southeastern Ordos Basin, China. Marine and Petroleum Geoloy, 91: 279–296.

ICCP, 1998. The new vitrinite classification (ICCP system 1994). Fuel, 77: 349–358.

ICCP, 2001. The new inertinite classification (ICCP System 1994). Fuel, 80: 459–471.

ISO 7404-2, 2009. Methods for the petrographic analysis of coals: Part 2: methods of preparing coal Samples, ISO 7404-2:2009(en); International Organization for Standardization. www.iso.org/standard/42832.html

ISO 7404-5, 2009. Methods for the petrographic analysis of coals: Part 5: methods of preparing coal Samples, ISO 7404-5:2009(en); International Organization for Standardization. www.iso.org/standard/42798.html

Jadoon, Q.H., Roberts, E., Blenkinsop, T., Wust, R., 2016. Organic petrography and thermal maturity of the Permian Roseneath and Muteree shales in the Cooper Basin, Australia. International Journal of Coal Geology, 154–155: 240–256.

Jerzykiewicz, J., 1987. Latest Carboniferous (Stephanian) and Early Permian (Autunian) palynological assemblages from the Intrasudetic Basin, southwestern Poland. Palynology, 11: 117–137.

Karnkowski, P., Pikulski, L., Wolnowski, T., 2010. Petroleum geology of the Polish part of the Baltic region – an overview. Geological Quarterly, 54: 143–158.

Kosakowski, P., Kotarba, M., Piestrzyński, A., Shogenova, A., Więcław, D., 2016. Petroleum source rock evaluation of the Alum and Dictyonema Shales (Upper Cambrian–Lower Ordovician) in the Baltic Basin and Podlasie Depression (eastern Poland). International Journal of Earth Sciences, 106: 743–761.

Körmösa, S., Bechtel, A., Sachsenhofer, R.F., Radovicsc, B.G., Milotac, K., Schubert, F., 2020. Petrographic and organic geochemical study of the Eocene Kosd Formation (northern Pannonian Basin): Implications for paleoenvironment and hydrocarbon source potential. International Journal of Coal Geology, 228: 103555.

Kus, J., Araujo, C.V., Borrego A.G., Flores D., Mendonca Filho, J.G., Hackley, P.C., Hamor-Vidó, M., Kalaitzidis, S., Kommeren, C.J., Kwiecińska, B., Mastalerz, M., Menezes, T.R., Misz-Kennan, M., Nowak, G.J., Petersen, H.I., Rallakis, D., Suarez-Ruiz, I., Sýkorová, I., Životić, D., 2017. Identification of alginite and bituminite in rocks other than coals: results of interlaboratory exercises of the Identification of Dispersed Organic Matter Working Group of the ICCP. International Journal of Coal Geology, 178: 26–38.

Lafargue, E., Marquis, F., Pillot, D., 1998. Rock-Eval 6 Applications in Hydrocarbon Exploration, Production, and Soil Contamination Studies. Revue l'Institute. Franais du Petrole, 53: 421–437.

Lewan, M.D., 1983. Effects of thermal maturation on stable organic carbon isotopes as determined by hydrous pyrolysis of Woodford Shale. Geochimica et Cosmochimica Acta, 47: 1471–1479.

Leventhal J., 1993. Metals and black shales. In: Organic Geochemistry (eds. M.H. Engel and S.A. Macko): 581–592. Principles and Applications, Plenum Press, New York.

Lin, L., Zhang, J., Li, Y., Jiang, S., Tang, X., Jiang, S., Jiang, W., 2013. The potential of China's lacustrine shale gas resources. Energy Exploration and Exploitation, 31: 317–335.

Liu, B., Bechtel, A., Sachsenhofer, R.F., Gross, D., Gratzer, R., Chen, X., 2017. Depositional environment of oil shale within the second member of Permian Lucaogou Formation in the Santanghu Basin, Northwest China. International Journal of Coal Geology, **175**: 10–25.

Liu, B., Bechtel, A., Gross, D., Fu, X., Li, X., Sachsenhofer, R.F., 2018. Middle Permian environmental changes and shale oil potential evidenced by high-resolution organic petrology, geochemistry and mineral composition of the sediments in the Santanghu Basin, Northwest China. International Journal of Coal Geology, **185**: 119–137.

Lojka, R., Drábková, J., Zajíc, J., Sýkorová, I., Franců, J., Bláhová, A., Grygar, T., 2009. Climate variability in the Stephanian B based on environmental record of the Mšec Lake deposits (Kladno–Rakovník Basin, Czech Republic). Palaeogeography, Palaeoclimatology, Palaeoecology, **280**: 78–93.

Lojka, R., Sýkorová, I., Laurin, J., Matysová, P., Matys Grygar, T., 2010. Lacustrine couplet-lamination: evidence for Late Pennsylvanian seasonality in central equatorial Pangaea (Stephanian B, Mšec Member, Central and Western Bohemian basins). Bulletin of Geosciences, **85**: 709–734.

Lorenc, S., 1993. Distribution, lithology and approximate geochemical features of the Sudetes black shales (in Polish with English summary). Prace Geologiczno-Mineralogiczne, **33**: 179–208.

Macellari, C., Whaley, J., 2019. The Vaca Muerta Formation: how a source became a reservoir. Geoexpro, **16**: 15–17.

Mansour, A., Gerslova, E. Sykorova, I., Vörös, D., 2020. Hydrocarbon potential and depositional paleoenvironmental of a Middle Jurassic succession in the Falak-21 well, Shushan Basin, Egypt: integrated palynological, geochemical and organic petrographic approach. International Journal of Coal Geology, **219**: 103374.

Martinek, K., Blecha, M., Daněk, V., Franců, J., Hladíková, J., Johnová, R., Uličný, D., 2006. Record of palaeoenvironmental changes in Lower Permian organic-rich lacustrine succession: Intragrated sedimentological and geochemical study of the Rudnik member, Krkonoše Piedmont Basin, Czech Republic. Palaeogeography, Palaeoclimatology, Palaeoecology, **230**: 85–128.

Mastalerz, K., 1990. Lacustrine successions in fault-bounded basins: 1 Upper Anthracosia Shale (Lower Permian) of the North Sudetic Basin, SW Poland. Annales Societatis Geologorum Poloniae, **60**: 75–106.

Mastalerz, K., Nehyba S., 1997. Comparison of Rotliegende lacustrine depositional sequences from the Intrasudetic, Northsudetic and Boskovice basins (Central Europe). Geologia Sudetica, **30**: 21–58.

Mastalerz, K., Wojewoda, J., 1988. Rotliegendes sedimentary basins in the Sudetes, central Europe. In: Workshop on Rotliegendes Lacustrine Basins, Książ Castle, 26–28 October 1988, Guidebook (ed. H. Kiersnowski): 1-9.

Mastalerz, M., Drobniak, A., Stankiewicz, A.B., 2018. Origin, properties and implications of solid bitumen in source-rock reservoirs: a review. International Journal of Geology, **195**: 14–36.

Mendonça Filho, J.G., Menezes, T.R., Mendonça, J.O., Oliveira, A.D., Silva, T.F., Rondon, N.F., Silva, F.S., 2012. Organic Facies: Palynofacies and Organic Geochemistry Approaches. Geochemistry – Earth's System Processes. Ed. Panagiotaras D., Intech Open Book Series: 211–248.

Mengying, L., Xinkai, C., 2021. A comparison of geological characteristics of the main continental shale oil in China and the U.S. Lithosphere, **1**.

Meyers, P.A., Pratt, L.M., Nagy, B., 1992. Geochemistry of metalliferous black shales. Chemical Geology, **99**: 1–211.

Miecznik, J.B., 1989. The Upper Silesian and Lower Autunian from NE limb of the Intta-Sudetic Depression (in Polish with English summary). Biuletyn Państwowego Instytutu Geologicznego, **363**: 5–40.

Mohamed, O., Mahdy, F., Sameh, S,. Tahoun, S.S., 2020. Palynofacies analysis and source rock evaluation of the Upper Cretaceous-Oligocene succession in the Drazia-1 well, Alamein Basin, Egypt. Arabian Journal of Geosciences, **11** (13), Iss. 22.

Ndip, E.A, Agyingi, C.M., Nton, M.E., Hower, J.C., Oladunjoye, M.A., 2019. Organic petrography and petroleum source rocks evaluation of the Cretaceous Mamfe Formation, Mamfe basin, southwest Cameroon. International Journal of Coal Geology, **202**: 27–37.

Nemec, W., Porębski, S., Teisseyre, A.K., 1982. Explanatory notes to the lithotectonic molasse profile of the Intra-Sudetic Basin, Polish Part. Veröffentlichungen des Zentralinstituts für Physik der Erde, Akademie der Wissenschaften der DDR, **66**: 267–278.

Nowak, G.J., 1998. Microscopic identification and classification of organic matter of the Upper Carboniferous Anthracosia Shales, Intra-Sudetic Depression, southwestern Poland. Geological Quarterly, **42**: 41–58.

Nowak, G.J., 2003. Petrology of organic matter dispersed in Late Palaeozoic sedimentary rocks of southwestern Poland (in Polish with English summary). Cuprum, **4** (29): 1–209.

Nowak, G.J., 2007. Comparative studies of organic matter petrography of the late palaeozoic black shales from Southwestern Poland. International Journal of Coal Geology, **71**: 568–585.

Nowak, G.J., Speczik, S., Oszczepalski, S., 2001. Petrographic composition of organic matter in the Kupferschiefer horizon of Poland. In: Mineral Deposits at the Beginning of the 21st Century (ed. A. Piestrzyński): 67–70. A.A. Balkena Publishers Lisse/Abingdon/Exto (PA)/Tokyo.

Obermajer, M., Foyer, M.G., Goodarzi, F., Snowdon, L.R. 1997. Organic petrology and organic geochemistry of Devonian black shales in southwestern Ontario, Canada. Organic Geochemistry, **26**: 229–246.

Oszczepalski, S., Nowak, G.J., Bechtel, A., Żák, K., 2002. Evidence for oxidation of the Kupferschiefer in the Lubin–Sieroszowice deposit, Poland: implication for Cu-Ag and Au-Pt-Pd mineralization. Geological. Quarterly, **46**: 1–23.

Panja, P., Velasco, R., 2018. Production of liquid hydrocarbons from shales. In: Encyclopedia of Petroleum Geosciences (ed. R. Sarhabi). Encyclopedia of Earth Sciences Series, Springer, Cham.

Peters, K.E., Cassa, M.R., 1994. Guidelines for evaluating source rocks geochemistry. AAPG Memoir, **60**: 93–120.

Pickel, W., Kus, J., Flores, D., Kalaitzidis, S., Christanis, C., Cardotte, B.J., Misz-Kennan, M., Rodriguesg, S., Hentschel, A., Hamor-Vido, M., Crosdale, P., Wagner, N., ICCP. 2017. Classification of liptinite – ICCP System 1994. International Journal of Coal Geolology, **169**: 40–61.

Pratt, L.M., 1984. Influence of paleoenvironmental factors on preservation of organic matter in Middle Cretaceous Greenhorn Formation, Pueblo, Colorado. AAPG Bulletin, **68**: 1146–1159.

Rimmer, S.M., Thompson, J.A., Goodnight, A.A., Robl, T.L., 2004. Multiple controls on the preservation of organic matter in Devonian-Mississipian marine black shales: geochemical and petrographic evidence. Palaeogeography, Palaeoclimatology, Palaeoecology, **215**: 125–154.

Robert, P., 1979. Classification des matieres organiques en fluorescence. Applications aux roches-meres petrolieres. Bulletin des Centres de Recherches Exploration-production Elf-Aquitaine, **3**: 223–263.

Robl, T.L Rimmer, S.M., Barron, L.S., 1992. Organic petrography of Mississipian and Devonian shales in east-central Kentucky. Fuel, **71**: 267–271.

Sachsenhofer, R.F., Bechtel, A., Reischenbacher, D., Weiss, A., 2003. Evolution of lacustrine systems along the Miocene Mur-Mürz fault system (Eastern Alps, Austria) and implications on source rocks in pull-apart basins. Marine and Petroleum Geology, **20**: 83–110.

Sanei, H., 2020. Genesis of solid bitumen. Scientific Reports, 10: 1559.

Scott, A.C., 2020. Fire: A Very Short Introduction. Oxford University Press.

Scott, A.C., 2022. Charcoalified vegetation from the Pennsylvanian of Yorkshire, England: Implications for the interpretation of Carboniferous wildfires. Review of Palaeobotany and Palynology, **296**: 104540.

Scott, A.C., Jones, T.P., 1994. The nature and influence of fire in the Carboniferous ecosystems. Palaeogeography, Palaeoclimatology, Palaeoecology, 106: 91–112.

Sliaupa, S., Sliaupienë, R., Zalũdienë, G., Vaskaboinikava, T., Bibikava, A., Evstratenko, L., Kovkhuto, A., 2016. Prospects of Lithuanian Silurian shale gas, Baltic sedimentary basin. Oil Shale 33: 357–372.

Speczik, S., Bechtel, A., Sun, Y.Z., Püttman, W., 1995. A stable isotope and organic geochemical study of the relationship between the Anthracosia Shale and Kupferschiefer mineralization (SE Poland). Chemical Geology, 123: 133–151.

Speczik, S., Oszczepalski, S., Nowak, G.J., Grotek, I., Niczyporuk, K., 2003. Organic matter alteration trends in the Polish Kupferschiefer: Ore genetic implications. Mineral exploration and Sustainable Development (ed. D. Eliopoulos). Millpress, Rotterdam.

Stach, E., Mackowsky M.-Th., Teichmüller, M., Taylor G.H., Chandra, D., Teichmüller, R. 1982. Textbook of Coal Petrology. 3rd edn. Gebrüder Borntraeger.

Stárková, M., Martínek, K., Mikuláš, R., Rosenau, N., 2015. Types of soft-sediment deformation structures in a lacustrine Ploužnice member (Stephanian, Gzhelian, Pennsylvanian, Bohemian Massif), their timing, and possible trigger mechanism. International Journal of Earth Sciences, 104: 1277–1298.

Suarez-Ruiz, I., Flores, D., Mendonca Filho, J.G., Hackley, P., 2012. Review and update of the applications of organic petrology: Part 1, geological applications. International Journal of Coal Geology, 99: 54–112.

Taylor, G.H., Teiichmüller, M., Davis, A., Diessel, C.F.K., Littke, R. Robert, R., 1998. Organic Petrology. Gebrüder Borntraeger. Berlin, Stuttgart.

Teichmüller, M., 1974. Über neue Macerale der Liptinit-Gruppe und die Entstehung von Micrinit. Fortschritte in der Geologie von Rheinland und Westfalen, 24: 37–64.

Teichmüller, M., Ottenjann, K., 1977. Art und Diagenese von Liptiniten und lipoiden Stoffen in einem Erdölmuttergestein aufgrund fluoreszenmikroskopischer Untersuchungen. Erdoel, Kohle, Petrochemie, 30: 387–398.

Trzepierczyńska, A., 1994. Microfloristic studies of the Ścinawka Dolna IG-1 borehole. In: Palaeogeography of the Upper Carboniferous and Lower Autunian deposits in the Nowa Ruda region (ed. A. Bossowski). Polish Geological Institute, Wrocław, Warszawa, NAG: 728/94 (unpubl. report).

Tyson, R.V., 1995. Sedimentary Organic Matter. Organic Facies and Palynofacies. Chapman and Hall, Londres.

Uglik, M., Nowak, G.J., 2015. Petrological recognition of bituminous inertinite enriched coals of the Lower Silesian Coal Basin (Central Sudetes, SW Poland). International Journal of Coal Geology, 139: 49–62.

Wyżykowski J., 1954. Preliminary report on the occurrence of Cu mineralization in the Intrasudetic Basin. Internal report. Polish Geological Institute, Warszawa, NAG: R/3584 (unpubl. report).

Yawanarajah, S.R., Kruge, M.A., Mastalerz, M., Śliwiński, W., 1993. Organic geochemistry of Permian organic-rich sediments from the Sudetes area, SW Poland. Organic Geochemistry, 20: 267–281.

Zang, W., Yang, W., Xie, L., 2017. Controls of organic matter accumulation in the Triassic Chang lacustrine shale of the Ordos Basin, central China. International Journal of Coal Geology, 183: 38–51.